Temporal Stability Analysis for the Evaluation of Spatial and Temporal Patterns of Surface Water Quality

Xiaobin Zhang
Zhejiang Academy of Agricultural Sciences
Ligang Ma
Xinjiang University
Yihang Zhu
Zhejiang Academy of Agricultural Sciences
Weidong Lou
Zhejiang Academy of Agricultural Sciences
Baoliang Xie
Zhejiang Academy of Agricultural Sciences
Li Sheng
Zhejiang Academy of Agricultural Sciences
Hao Hu
Zhejiang Academy of Agricultural Sciences
Kefeng Zheng
Zhejiang Academy of Agricultural Sciences
Qing Gu (guq@zaas.ac.cn)
Zhejiang Academy of Agricultural Sciences https://orcid.org/0000-0003-1455-0743

Research Article

Keywords: water quality, temporal stability, water management, monitoring network, spatial pattern

Posted Date: May 10th, 2021

DOI: https://doi.org/10.21203/rs.3.rs-291728/v1

Version of Record: A version of this preprint was published at Water Resources Management on February 22nd, 2022. See the published version at https://doi.org/10.1007/s11269-022-03090-8.

Temporal stability analysis for the evaluation of spatial and temporal patterns of surface water quality

Xiaobin Zhang[1,2], Ligang Ma[3], Yihang Zhu[1], Weidong Lou[1], Baoliang Xie[1], Li Sheng[1,2], Hao Hu[1,2], Kefeng Zheng[1,2], Qing Gu[1,2,*]

[1] Institute of Digital Agriculture, Zhejiang Academy of Agricultural Sciences, Hangzhou 310021, China

[2] Key Laboratory of Information Traceability for Agricultural Products, Ministry of Agriculture and Rural Affairs of China, Hangzhou 310021, China

[3] College of Resource and Environmental Science, Xinjiang University, Urumqi 830046, China

*Corresponding author at: Institute of Digital Agriculture, Zhejiang Academy of Agricultural Sciences, Hangzhou 310021, China. E-mail address: guq@zaas.ac.cn (Q. Gu)

Abstract

Better characterizing the spatio-temporal pattern of water quality would increase the ability to effectively manage water resources. This study applied the concept of temporal stability analysis (TSA) to explore the temporal characteristics of spatial variability in surface water quality. Monitoring data from 41 monitoring stations in Qiantang River, China for 2017-2019 were used to assess four indicators: dissolved oxygen (DO), permanganate index (COD_{Mn}),

total phosphorus (TP), and ammonia nitrogen (NH_3–N). A Spearman's rank correlation for each pair of monitoring times demonstrated that the spatial pattern of water quality was maintained for a specific period of time. The TP concentration was most temporally stable compared with the other three indicators across the study area. A temporal analysis of relative differences was applied to examine the temporal stability of the sampling sites. The mean concentrations, with acceptable errors, were estimated from the representative sites identified for the four water quality indicators. Different metrics were assessed to identify the temporally stable sites. The standard deviation of the relative difference (SDRD) and index of temporal stability (ITS) were found to be better for identifying the stable sites compared to the mean absolute bias error (MABE) and root mean square error (RMSE) in this study. A correlation analysis between the temporal stability indices and potential influencing factors showed that land use proportions (forest, built-up land, and agricultural land), and socio-economic indicators (gross domestic product [GDP] and population density) were closely associated with the temporal stability of water quality. The results showed evidence that the TSA method was feasible and effective in identifying the temporal stability of surface water quality and optimizing the water quality monitoring program. This study's method and findings can help improve surface water quality monitoring strategies and water resource management.

Keywords: water quality; temporal stability; water management; monitoring network; spatial pattern

1 Introduction

Monitoring surface water quality is critical for regulating and managing water resources. The water monitoring network is important for evaluating, preserving, and remediating water quality (Ouyang, 2005). Recent significant advances in communication and sensor technology have greatly improved the ability to monitor surface water quality (Glasgow et al., 2004), and the real-time remote monitoring network for surface water quality has become essential for water resource management (Nasirudin et al., 2011; Quinn et al., 2010; Storey et al., 2011). Unfortunately, many surface water quality monitoring networks have been developed without a deliberate design (Strobl and Robillard, 2008), which may lead to incorrect decisions and wasted resources. In addition, the installation, operation, and maintenance of monitoring networks are expensive and require considerable human labor (Storey et al., 2011). Properly designing monitoring systems is vital for monitoring water quality and managing water resources.

There are many challenges in developing an effective water quality monitoring network, including selecting indicators, identifying representative monitoring sites, and determining adequate sampling frequencies (Behmel et al., 2016; Dixon et al., 1999; Strobl and Robillard, 2008). High priority has been placed on researching approaches that decrease the number of observations, without significant information loss (Behmel et al., 2016; Ouyang, 2005). The ideal approach is to permanently monitor important water quality indicators at fixed stations representing the water quality levels in the area of interest with optimal and representative temporal frequencies (Strobl and Robillard, 2008). However, water quality usually varies significantly over time and space; this variability needs to be considered in designing a

monitoring program. Many researchers have reported that characterizing the spatio-temporal pattern of water quality can greatly advance our ability to regulate water quality (Gu et al., 2015; Su et al., 2011). Temporally continuous monitoring data over a specific territory should be used to characterise the spatio-temporal patterns of water quality and to determine the important indicators, representative sampling sites, and adequate sampling frequencies. This knowledge helps designers improve strategies for monitoring surface water quality and corresponding water resource management policies.

Many techniques have been developed to optimize water quality monitoring programs. Clustering methods have been widely used to explore the spatio-temporal patterns of water quality. These methods include the cluster analysis (CA) (Gu et al., 2015; Hussain et al., 2008), genetic algorithm (GA) (Al-Zahrani and Moied, 2003; Icaga, 2005), and self-organizing map (SOM) (Kohonen, 1990; Zhou et al., 2016). Clustering approaches classify the monitoring stations or times based on similarities in water quality measures. Similar management policies can be applied to the monitoring sites in the same group. Alternatively, representative stations or specific times can be selected for each group to reduce the number of observations (Park et al., 2014). Principal component analysis (PCA) has been widely used to identify possible pollution sources and the contribution of these sources to the variability in water quality (Ouyang, 2005; Su et al., 2011). These methods can reveal either temporal or spatial patterns with respect to water quality, but cannot characterize the temporal characteristics of the spatial patterns. This is because they use only mean concentrations or one period of data to classify the monitoring sites/times or to identify the important water quality indicators.

The concept of temporal stability analysis (TSA) was proposed by Vachaud et al. (1985) to investigate the temporal characteristics of the spatial variability of soil water content. This method was proposed as a way to reduce the number of field observations, by selecting a few representative locations. Many studies have confirmed the usefulness of the time stability approach. The approach has been widely used to identify the most stable sampling sites for representing the mean soil moisture conditions in a specific area (Cosh et al., 2006; Dorigo et al., 2011; Martínez-Fernández and Ceballos, 2003; Neves et al., 2017; Sur et al., 2013; Zhang and Shao, 2013; Zhou et al., 2007). Many studies have used TSA to validate and calibrate the remote sensing of soil moisture (Colliander et al., 2017; Cosh et al., 2004; Cosh et al., 2008; Crow et al., 2012; Jackson et al., 2012; Peng et al., 2017; Wagner et al., 2008). Other studies have expanded the application of TSA method to explore the temporal stability of other observations. For example, Stocker et al. (2018) and Pachepsky et al. (2018) applied TSA to investigate the temporally stable patterns of *Escherichia coli* concentrations in water sediment. Ran et al. (2015) applied TSA to select optimal groundwater level monitoring locations to improve a groundwater monitoring network. Douaik et al. (2006) used TSA to assess the temporal characteristics of soil salinity spatial patterns to optimize a sampling strategy. These studies showed that the TSA method has promising potential for investigating the temporal stability of spatial pattern of variable field measurements, and for optimizing the observation scheme.

This study applied TSA to surface water quality measurements to assess the spatio-temporal variabilities of the concentrations. The most representative sampling sites were selected to estimate mean concentrations across the study area. There were three

specific study objectives. The first was to characterize the temporal stability of the spatial pattern of four surface water quality indicators: dissolved oxygen (DO), permanganate index (COD_{Mn}), total phosphorus (TP), and ammonia nitrogen (NH_3–N). The second objective was to identify the best temporally-stable water quality sampling sites to represent the areal mean for the study area. The third objective is to relate the influencing variables, such as land use indicators, GDP, and elevation, with the temporal stabilities of the water quality concentrations and identify the important variables influencing the temporal stabilities.

2 Materials and methods

2.1 Study area and water quality data

The monitoring stations were distributed in Qiantang River and its tributaries in Zhejiang Province, one of the most rapidly developing regions in eastern China (Fig. 1). The Qiantang River is the largest river in Zhejiang, and plays an important role in socio-economic development. The main path of the Qiantang River is 668 km long, with a basin area of 48,000 km^2. This area accounts for 47% of the province area. The average annual total water storage capacity in the Qiantang River basin is 38.9 billion m^3. The mountainous-hilly region accounts for 70.5% of the basin area; built-up land covers 7.5% of the area; arable land occupies approximately 17.1% of the area; and rivers and lakes make up approximately 4.8% of the area. According to the Zhejiang water resources bulletin in 2018, there is a lack of optimism about the overall water quality in Qiantang River. The upstream water quality was significantly better than downstream water quality; NH_3–N, COD_{Mn}, and TP were the main pollution indicators. Fig. 1 shows the sampling site locations.

Monthly reports from September 2017 to August 2019 were collected from 41 monitoring stations along the Qiantang River and its tributaries. The data were collected from the automatic monitoring network of surface water quality in Zhejiang Province. Water quality measurements were collected using environmental quality standards for surface water in China (GB3838-2002) (EPB, 2002) and technical specifications for surface water and wastewater monitoring (Qi, 2006). No data were missed during the study period. The specified methods were as follows: DO, the membrane electrode method; COD_{Mn}, the acidic potassium permanganate method; TP, the spectrophotometric method; NH_3–N, the spectrophotometric method with salicylic acid.

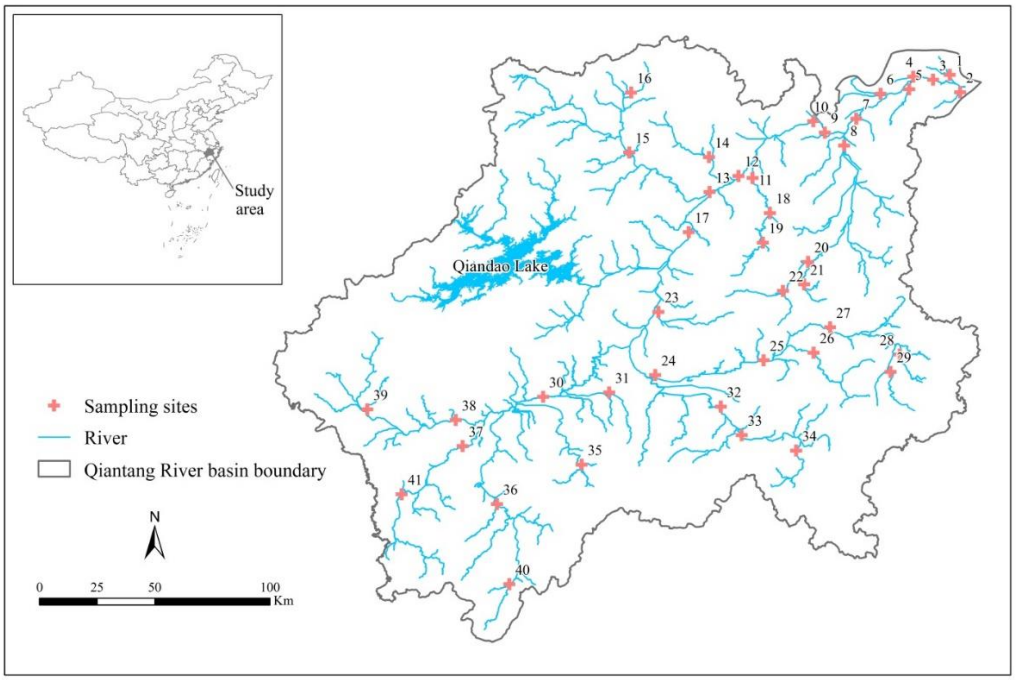

Fig. 1 Location of the study area in China and spatial distribution of the monitoring sites.

148 *2.2 Methods*

149 2.2.1 Temporal stability analysis (TSA)

150 TSA was originally proposed as a method for analyzing the temporal variability of spatial
151 distributions of measured soil water data (Vachaud et al., 1985). It has been widely applied in
152 soil moisture studies. Two techniques were used to evaluate temporal stability: the
153 Spearman's rank correlation test and a temporal analysis of relative difference. The
154 nonparametric correlation test was used to investigate the stability of site ranks between
155 different sampling times. This test can be expressed as:

156 $$r_s = 1 - \frac{6\sum_{i=1}^{n}\left(R_{ij} - R_{ij'}\right)^2}{n(n^2-1)} \quad (1)$$

157 In this expression, R_{ij} and $R_{ij'}$ are the ranks of observed values at site i at sampling times
158 j and j'. The variable n is the number of sampling sites. An r_s value of zero indicates that
159 there is no temporal stability in the site ranks between two sampling times. An r_s value close
160 to one indicates that the site ranks persists over time; a value of one reflects absolute
161 persistence. Correlation coefficients were calculated for each water quality indicator for all
162 possible survey combinations. The mean coefficient values were calculated for each time lag
163 to identify the time-associated drift in temporal stability. The time lag was defined as the
164 interval between the sequence numbers between two sampling periods. For example, there is
165 a time lag of one between September and October, and there is a time lag of three between
166 September and December. The smallest time lag was one, and the largest time lag was 11.
167 This reflected the total of 12 sampling periods in this study.

168 Relative difference (RD) is used to calculate the metrics that examine the temporal stability
169 of sampling locations. RD is calculated based on the differences between concurrent

individual measurements and spatial average values. RD is expressed as:

$$\delta_{ij} = \frac{S_{ij} - \bar{S}_j}{\bar{S}_j} \quad (2)$$

In this expression, S_{ij} is the observation at location i at sampling time j. The variable $\bar{s}_j$ is the average value at time j, and is calculated as:

$$\bar{S}_j = \frac{1}{n}\sum_{i=1}^{n} S_{ij} \quad (3)$$

The mean relative difference (MRD) and standard deviation of the relative difference (SDRD) were used to identify the temporal stability of sampling sites. The variables MRD ($\bar{\delta}_i$) and SDRD ($\sigma(\delta_i)$) are defined as follows based on the relative difference:

$$\bar{\delta}_i = \frac{1}{m}\sum_{j=1}^{m} \delta_{ij} \quad (4)$$

$$\sigma(\delta_i) = \sqrt{\frac{(\delta_{ij} - \bar{\delta}_i)^2}{m-1}} \quad (5)$$

In this expression, m is the number of surveys. Monitoring sites with MRD values close to zero can be used to represent the mean water quality concentrations across the study area. A lower SDRD value indicates better temporal stability. MRD and SDRD were used in combination to identify the representative monitoring locations for the spatially time-stable average measurements, with MRD near zero and with the lowest values of SDRD.

Three indices, which combined MRD and SDRD, were applied to examine temporal stability. The index of temporal stability (ITS) was used to quantify the temporal stability of locations (Jacobs et al., 2004). The monitoring location with smallest ITS was identified as the most temporally stable site (Zhao et al., 2010). The mean absolute bias error (MABE) (Hu et al., 2010) and root mean square error (RMSE) (Gao et al., 2013) were applied as an offset to adjust the estimation errors. The sites with lower values of MABE or RMSE generally had higher temporal stability. The ITS at site i is calculated as:

$$ITS_i = \sqrt{\bar{\delta}_i^{\,2} + \sigma(\delta_i)^2} \quad (6)$$

The MABE is calculated using the following equation:

$$MABE_i = \frac{1}{m}\sum_{j=1}^{m}\left|\frac{\delta_{ij}-\bar{\delta}_i}{1+\bar{\delta}_i}\right| \quad (7)$$

The RMSE of the predicted water quality concentrations is calculated as:

$$RMSE_i = \sqrt{\frac{1}{m}\sum_{j=1}^{m}\left(\frac{S_{ij}}{1+\bar{\delta}_i} - \frac{S_{ij}}{1+\delta_{ij}}\right)^2} \quad (8)$$

2.2.2 Evaluation and validation

A Pearson correlation analysis was used to evaluate the goodness-of-fit between measurement and predicted mean water quality concentrations with two metrics: correlation coefficient (*r*) and root mean square error (RMSE). To validate the representativeness of the selected monitoring sites, the data were split into two groups. The first group included data from September 2017 to August 2018, which were used for TSA and representative site identification. The second group included data from September 2018 to August 2019, which were used for validation. A Pearson correlation analysis was also used to investigate the relationships between the temporal stability indices and potential influencing factors. The Pearson correlation analysis was performed at p=0.01 and p=0.05 significance levels using a 2-tailed test; testing was performed using the Statistical Product and Service Solutions (SPSS) software (version 20.0; SPSS Inc, Chicago, IL, USA).

2.3 Influencing factors

The spatio-temporal variability of surface water quality is driven by different environmental and socio-economic variables, including adjacent land use pattern,

topographic features, economic development condition, and meteorological factors (Gu et al., 2014; Gu et al., 2015). To identify the important variables influencing the temporal stabilities, the study evaluated four land use indicators (forest, built-up land, agricultural land, and water proportions), two socio-economic indicators (GDP and population density), elevation, and precipitation. These indicators were correlated with the temporal stability indicators associated with water quality. The land use parameters were calculated using a digital land use map for 2018. Land use was classified into five categories: forest, built-up land, agricultural land, water, and other land use types (Fig. 2). A digital elevation model (DEM) (30 m) was used to delineate the sub-watershed boundaries in the Qiantang River watershed using ArcGIS 10.0 software (ESRI, Redlands, CA, USA). The sub-watershed layer was laid over the land use map to calculate the land use type proportions in the sub-watersheds, where the monitoring stations are located.

Topographic features in the study area were represented by elevation, which significantly influences hydrological characteristics (Yu et al., 2016). Elevation was extracted from the DEM data in ArcGIS. For the socio-economic conditions, county-scale GDP and population density data were obtained from the Zhejiang Statistical Yearbook (2018). The GDP and population in the sub-watershed were calculated from the county-scale data, based on the areal proportions. Precipitation data were downloaded from the China Meteorological Data Sharing Service System. There are 7 meteorological monitoring stations within the study area. We applied the Kriging interpolation method to extend the precipitation values. The average values across the sub-watersheds were extracted for analysis.

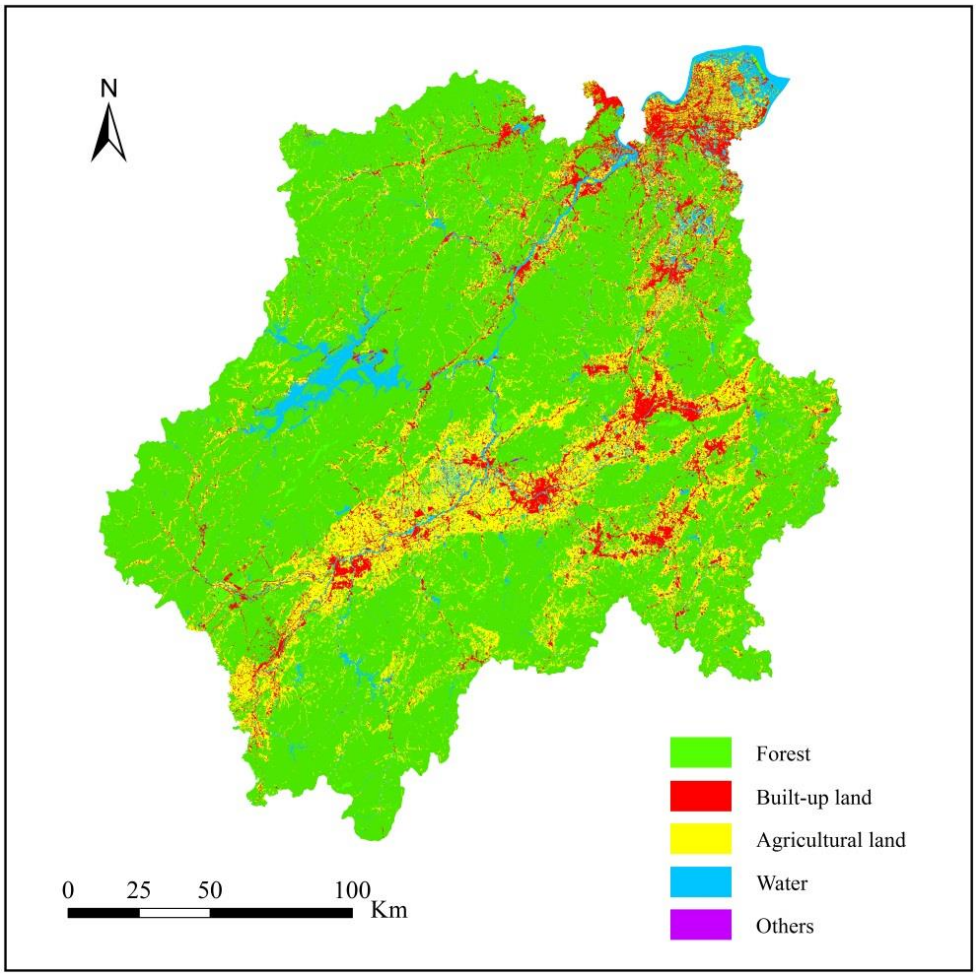

Fig. 2 Land use in the Qiantang River basin in 2017.

3 Results and discussion

3.1 General statistical characteristics of the water quality

Table 1 and Fig. 3 show statistics for water quality concentrations and annual variation, respectively. There were no monotonic temporal trends for the water quality indicators. The mean DO concentrations increased from September 2017 to February 2018. This was followed by a decrease, and then by relatively stable levels after May 2018. The mean NH_3-N showed a similar trend over time as the average DO concentrations. The highest mean DO concentration and the lowest mean COD_{Mn} and TP values were in February 2018. As such,

this month may have experienced the best water quality conditions from September 2017 to August 2018. The variabilities of concentrations were large, as demonstrated by the high CVs (coefficients of variation, the last column in Table 1), which ranged from 28.44% to 76.95%. The DO had the lowest spatial variability, as indicated by the smallest CV. NH_3-N had a larger CV compared to the other indicators, presenting the largest spatial variability. According to China's surface water quality standards (GB3838-2002) (EPB, 2002), the mean DO value achieved the first grade of the standards, while COD_{Mn}, TP, and NH_3-N reached the second grade.

Table 1 Statistics for water quality concentrations between September 2017 and August 2019 for 41 monitoring stations along the Qiantang River.

Water quality indicators	**Minimum**	**Maximum**	**Mean**	**S.D.**	**CV (%)**
DO (mg/L)	1.64	13.95	7.84	2.23	28.44
COD_{Mn} (mg/L)	0.90	5.50	2.89	1.03	35.57
TP (mg/L)	0.005	0.252	0.099	0.057	57.45
NH_3-N (mg/L)	0.02	1.05	0.29	0.23	76.95

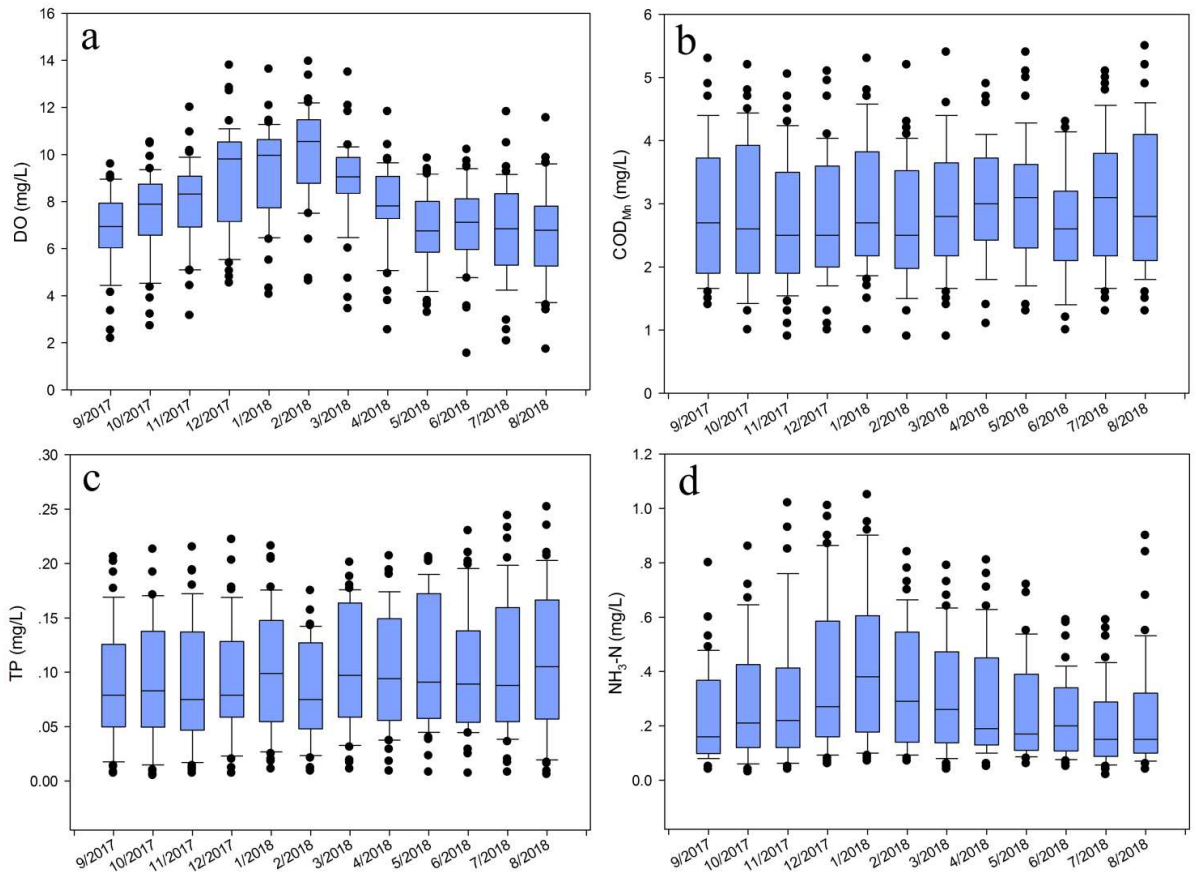

Fig. 3 Annual variations in (a) DO, (b) COD_{Mn}, (c) TP, and (d) NH_3-N between September 2017 and August 2018.

3.2 Temporal stability analysis

3.2.1 Spearman's rank correlation (r_s)

Fig. 4 shows the matrixes of the Spearman's rank correlation coefficients in terms of 12-month comparisons. All pairs were significantly correlated at the 0.01 probability level, indicating a strong temporal persistence in the ranks of the water quality indicators from the monitoring sites. This was consistent with the strong temporal stabilities identified in the spatial patterns of soil water content (Sur et al., 2013; Wagner et al., 2008), *Escherichia coli* concentrations in water sediment (Pachepsky et al., 2018; Stocker et al., 2018), groundwater

level (Ran et al., 2015), and soil salinity (Douaik et al., 2006). The significance analysis showed that the Spearman's correlation coefficients of COD_{Mn} and NH_3-N did not significantly differ. In contrast, the other pairs of the water quality indicators significantly differed at $p < 0.01$, with means of 0.68, 0.8, 0.88, and 0.82 for DO, COD_{Mn}, TP, and NH_3-N, respectively. The higher coefficients for TP indicated that its concentration tended to be more temporally stable compared with the other three indicators across the study area.

The correlations presented time-related drift, as demonstrated by the smaller values of coefficients as the time lags increased (Fig. 5). This indicated that the spatial patterns of water quality can be maintained for short periods but cannot be sustained for long periods. Similar findings have been reported in the studies on soil moisture (Sur et al., 2013; Zhang and Shao, 2013) and other measurements (Douaik et al., 2006; Ran et al., 2015; Stocker et al., 2018). Moreover, the drift effect appeared to differ among the four water quality indicators. Fig. 4 shows that the DO showed the largest decrease in the mean coefficient (0.28) as the time lag extended from 1 to 11. The TP value experienced the smallest decrease in coefficient (0.11). This was consistent with the coefficient means, and showed that the spatial pattern of TP concentrations can remain longest and DO concentrations had the lowest temporal stability.

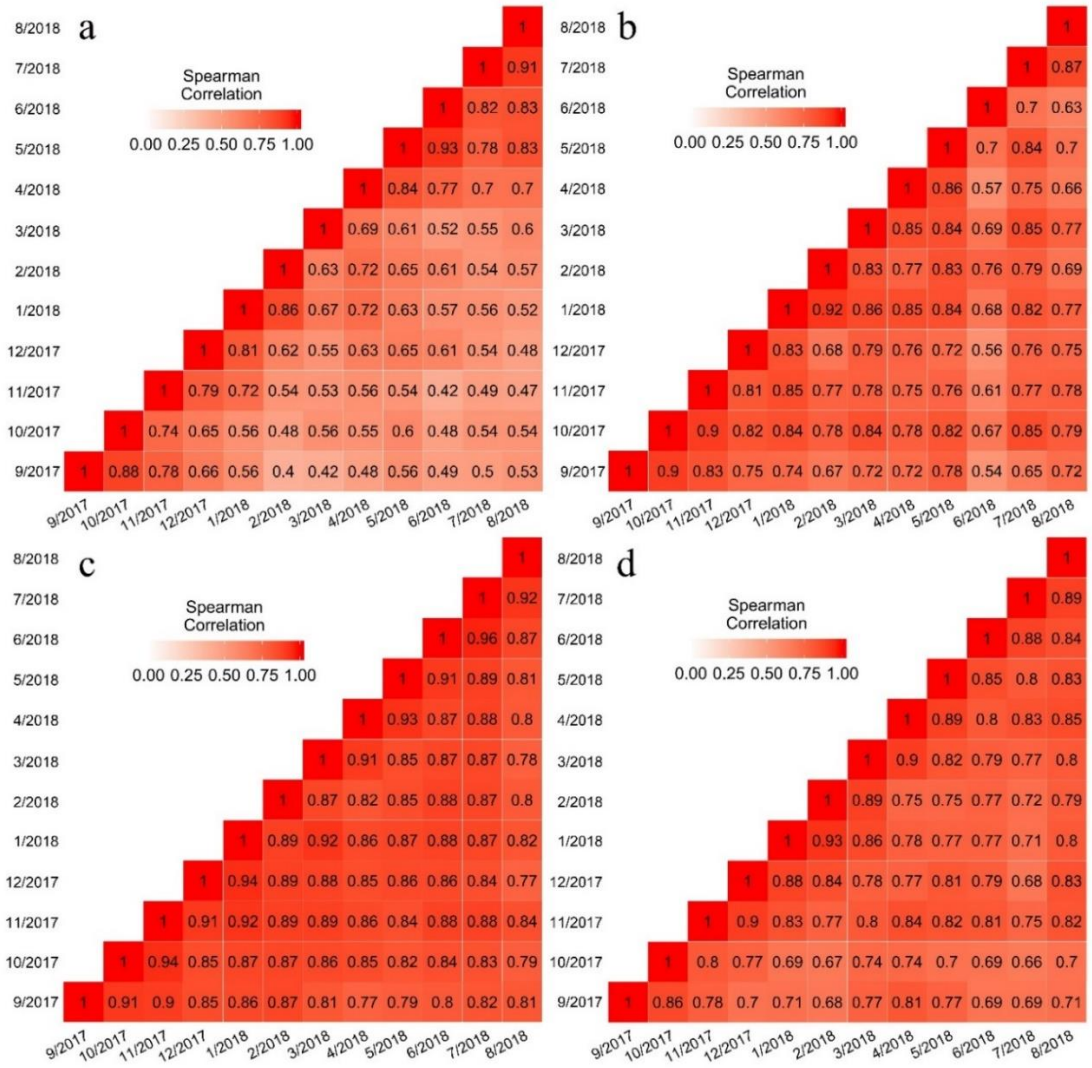

287

288 **Fig. 4 Matrix of Spearman's rank correlation coefficients for the comparisons of water**

289 **quality concentrations in different months** between September 2017 and August 2018**:** (a)

290 DO, (b) COD_{Mn}, (c) TP, and (d) NH_3-N**.** All correlations are statistically significant ($p<0.01$).

291

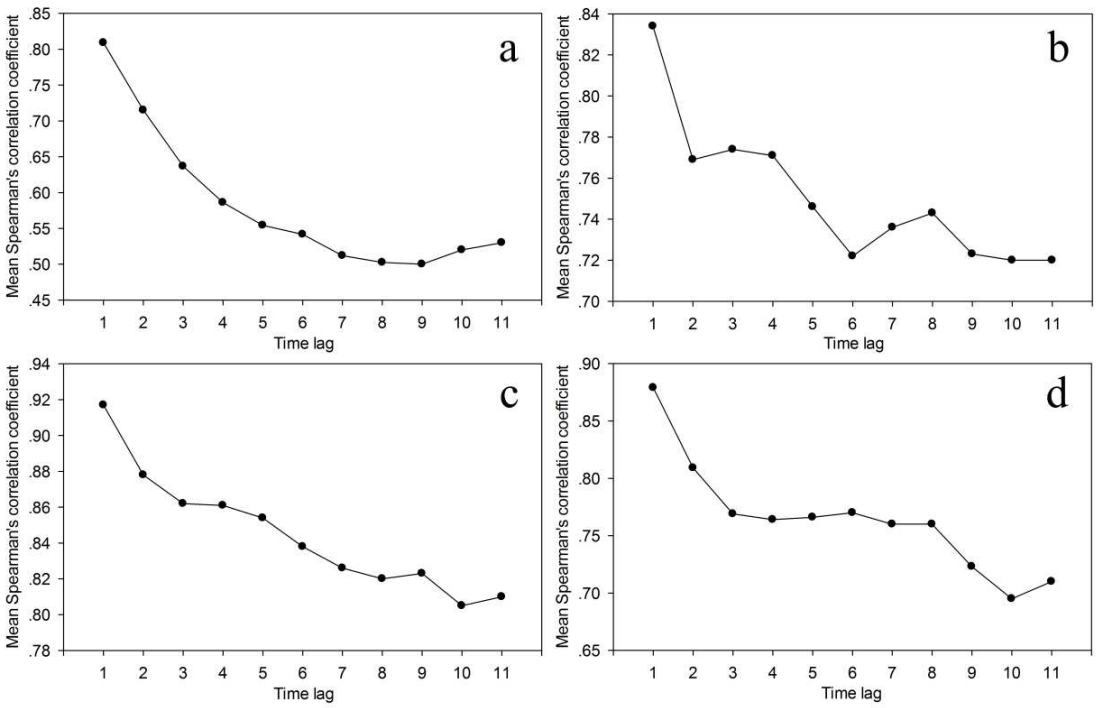

Fig. 5 Mean Spearman's rank correlation coefficient corresponding to different time lags (months) for (a) DO, (b) COD_{Mn}, (c) TP, and (d) NH_3-N.

3.2.2 MRD and SDRD

Fig. 6 shows the ranking of MRDs from lowest to highest. The bars show the associated SDRDs. Sampling sites with higher MRDs had consistently higher concentrations compared to the mean values. The range of MRD value was 86.58% (-54.17% to 32.41%) for DO, 113.31% (-58.58% to 54.73%) for COD_{Mn}, 185.15% (-91.33% to 93.82%) for TP, and 196.04% (-76.6% to 119.44%) for NH_3-N. The larger ranges of MRDs for COD_{Mn} and TP were associated with a stronger spatial variability in the concentrations. The MRD values were asymmetric, particularly for DO and NH_3-N. DO tended to have more MRD values larger than 0, while NH_3-N had more values smaller than 0. This indicated there were more sites with water quality values that were better than mean levels, based on the DO and NH_3-N

concentrations. SDRD values varied significantly, ranging from 4.05% to 39.56% for DO, from 5.29% to 37.5% for COD_{Mn}, from 2.12% to 44.42% for TP, and from 7.24% to 77.56% for NH_3-N.

Fig. 7 shows the relationships between the MRD and SDRD. MRD was significantly positively correlated with SDRD for COD_{Mn}, TP, and NH_3-N ($p < 0.01$, Pearson test). In contrast, the MRD was not correlated with SDRD for DO. With respect to representing the mean water quality in the study area, the results indicated that the sampling sites with lower COD_{Mn}, TP, and NH_3-N concentrations were more stable compared to sites with higher concentrations.

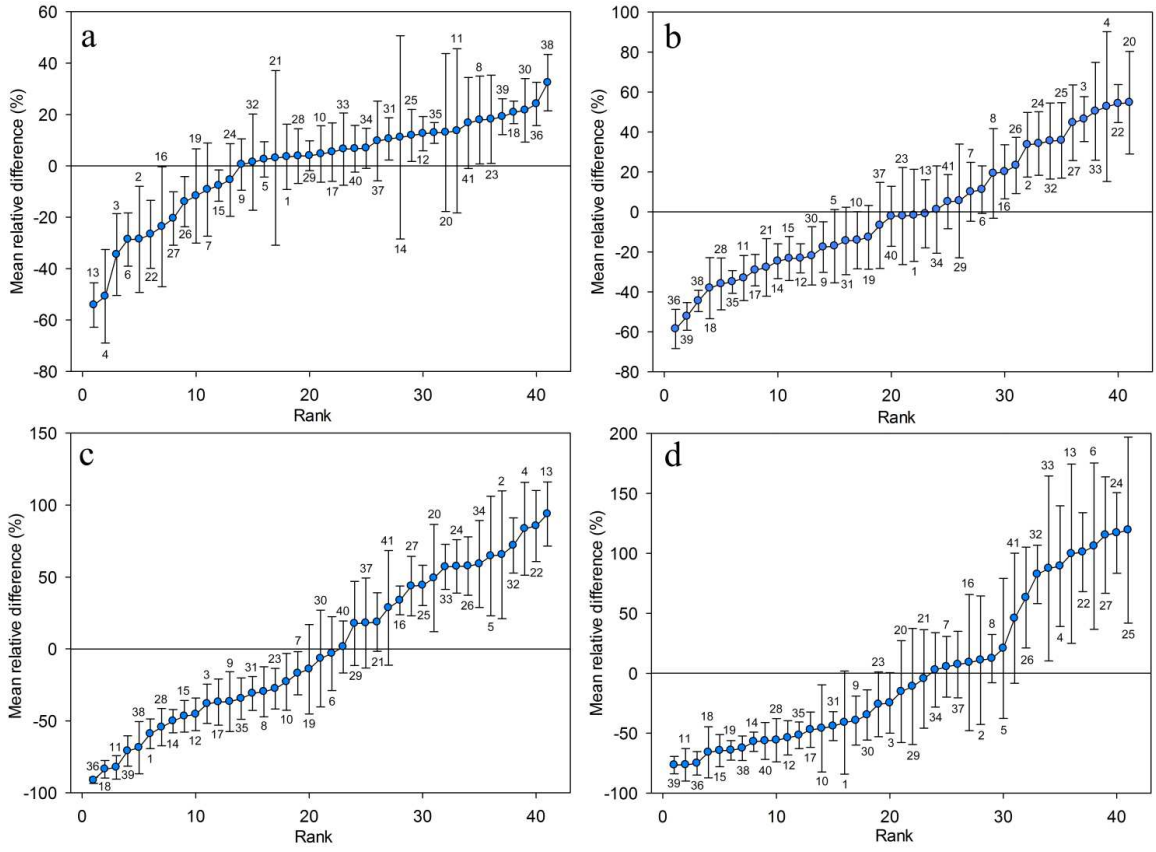

Fig. 6 The mean relative difference (MRD) and standard deviation of relative difference (SDRD) of (a) DO, (b) COD_{Mn}, (c) TP, and (d) NH_3-N. The MRDs are ranked in ascending

order; the associated SDRD values are indicated by error bars. The numbers near the bars are the identification numbers of the monitoring sites.

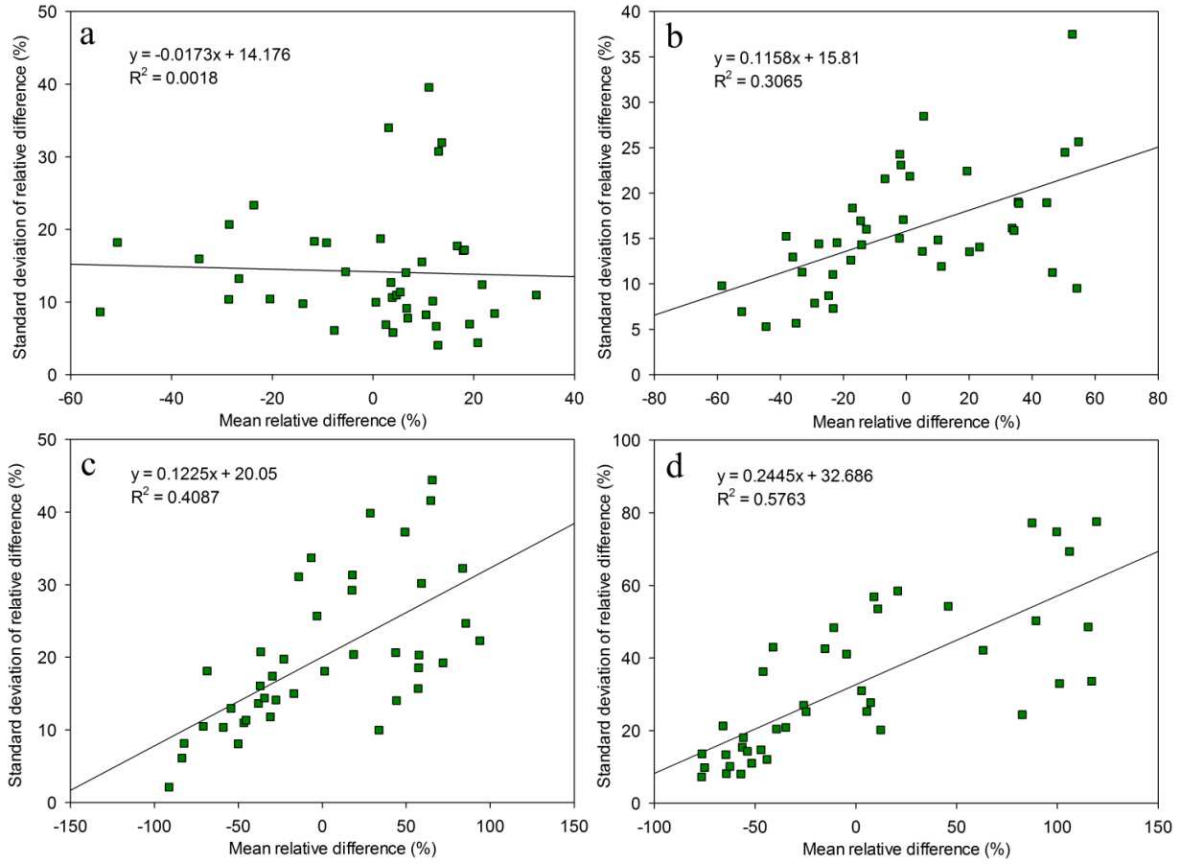

Fig. 7 Relationships between the mean relative difference (MRD) and standard deviation of relative difference (SDRD) for (a) DO, (b) COD_{Mn}, (c) TP, and (d) NH_3-N.

3.3 Identification and validation of representative sampling sites

To identify representative monitoring locations, it is important to define the criteria for selecting them. Several criteria have been proposed for different case studies to support the temporal stability analysis technique. For example, Vachaud et al. (1985) selected the location with the lowest SDRD value as the most temporally stable site. Grayson and Western

(1998) selected representative sampling stations based on the closeness of the relative difference to zero. Van and Wierenga (2001) considered locations as estimators of the mean soil moisture for a given network, by setting 5% as the threshold for the standard deviation at a small spatial scale (1 ha). In this study, the monitoring sites were distributed over a broad territory. This resulted in high temporal variation. We chose four indices to identify the representative monitoring sites based on the TSA method: SDRD, ITS, MABE, and RMSE.

Table 2 shows the representative sites identified using SDRD, ITS, MABE, and RMSE for the four water quality indicators. The representative water quality concentrations were linked to the mean values of all sampling sites. A subset of the identified stations represented the sites with mean concentrations with acceptable errors. For DO, the results from the representative sites identified by the four indices were all significantly correlated with the mean concentration (p<0.01). Site 35 resulted in the best estimates of the mean value using SDRD. For COD_{Mn}, site 38 was identified using both SDRD and MABE, and site 39 was selected using RMSE. Site 38 and site 39 showed an equal correlation coefficient, and were both closely associated with the mean value (p<0.05). For TP and NH_3-N, only the locations determined using ITS (site 40 for TP and site 8 for NH_3-N) were effectively associated with the regional mean concentrations. This was because the SDRD values were closely related to the MRD values, and the locations with smallest SDRDs did not correspond to the sites with MRD values close to zero. The use of MABE and RMSE values resulted in the selection of the same sites (site 13 for DO, site 36 for TP, and site 39 for NH_3-N) for all the water quality indicators except COD_{Mn}. According to the results, if the MRD and SDRD values are closely correlated, MABE and RMSE methods tend to produce the same representative locations as

353 SDRD. This was the case for the water quality indicators TP and NH_3-N. However, these
354 locations may not effectively represent the regional means. The identified locations differed
355 for the four water quality indicators, indicating that these indicators are likely to show
356 different characteristics with respect to temporal consistency.

357 Fig. 8 shows the comparison of water quality concentrations between the total mean values
358 and the concentrations of the four indicators at representative sites, using data from
359 September 2018 to August 2019 for validation. The selected sites resulted in mean
360 concentrations that had acceptable errors. Site 35, identified using SDRD for DO, produced
361 the best estimates of the mean concentration. This was followed by site 40 for TP and site 8
362 for NH_3-N. The representative site for COD_{Mn} had the lowest correlation with the mean
363 concentration.

364

365

366

367

368

369

370

371

372

373 **Table 2** Pearson correlation coefficients and RMSEs for the mean concentrations and the

374 concentrations at the single site identified by four temporal stability indices.

Water quality indicator	Method	Representative site	*r*	RMSE
DO	SDRD	35*	0.986 "	0.21
	ITS	29	0.956 "	0.36
	MABE	13	0.765 "	0.78
	RMSE	13	0.765 "	0.78
COD_{Mn}	SDRD	38*	0.669′	0.104
	ITS	41	0.488	0.122
	MABE	38	0.669′	0.104
	RMSE	39	0.669′	0.104
TP	SDRD	36	0.458	0.029
	ITS	40*	0.715′	0.0089
	MABE	36	0.458	0.029
	RMSE	36	0.458	0.029
NH_3-N	SDRD	39	0.494	0.136
	ITS	8*	0.722′	0.054
	MABE	39	0.494	0.136
	RMSE	39	0.494	0.136

375 * Sites resulted in the best estimates of mean concentrations.

376 ′ $p < 0.05$

377 " $p < 0.01$

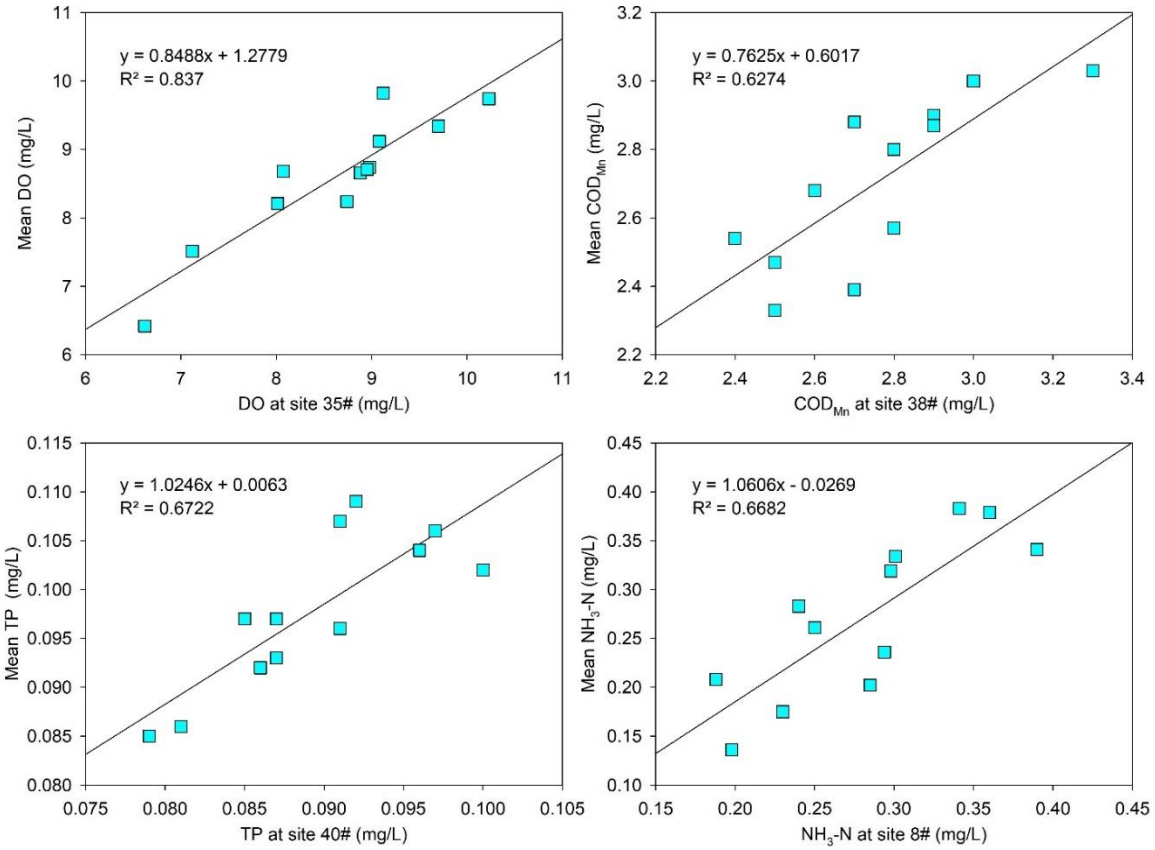

Fig. 8 Comparison of water quality concentrations between the total mean values and concentrations of representative sites for DO (site 35), COD_{Mn} (site 38), TP (site 40), and NH_3-N (site 8), between September 2018 and August 2019.

3.4 Influencing factors for temporal stability analysis

A Pearson correlation analysis was used to assess the influence of different factors (land use, socio-economic status, topography, and precipitation) on the temporal stabilities of the water quality measures. Table 3 shows the correlations between MRD, SDRD, and ITS and the potential factors. SDRD and ITS were found to be better than MABE and RMSE for identifying representative sites in this study, so we excluded MABE and RMSE from the process of identifying the influencing factors.

Forest land use (%) was significantly positively correlated with the MRD of DO and was significantly negatively correlated with MRD values of COD_{Mn}, TP, and NH_3-N. There were negative relationships between forest (%) and the SDRD values of TP and NH_3-N. Built-up land (%) showed a significant negative correlation with the MRD value of DO. There were weak positive relationships with MRDs for COD_{Mn} and TP. There were significantly positive correlations with MRD and SDRD for NH_3-N. Agricultural land (%) was negatively related to MRD and was positively related to ITS for DO. There were positive correlations with MRDs and SDRDs for COD_{Mn}, TP, and NH_3-N. Water land use (%) was positively associated with the MRD of DO and was negatively related to ITS of COD_{Mn}.

Many studies have reported a close relationship between land use and water quality (Bu et al., 2014; Lee et al., 2009; Meneses et al., 2015). Previous studies showed that construction land and cultivated land have a negative impact on surface water quality. In contrast, woodland has a positive influence on water quality. In this study, the land use proportions were closely related to temporal stability indices, which were generally consistent with the relationships between land use type proportions and water quality concentrations. Water quality tended to be more stable in the areas where there were higher proportions of forest land and lower proportions of built-up land and agricultural land. Forest land can stabilize the nearby water quality, because it significantly contributes to soil and water conservation and water purification (Gu et al., 2019). Built-up land and agricultural activities increase pollution risks for adjacent water and can increase water quality fluctuations. Water itself has the ability to purify itself, so it is reasonable for water to contribute to the stability of water quality.

GDP and population density are important socio-economic indicators, and are closely associated with human activities and surface water quality (Gu et al., 2014; Wu and Chen, 2013). Table 3 shows that GDP and population density had important impacts on the temporal stability of water quality. This is indicated by the close relationships with the temporal stability indices. Regions with higher GDP and population density tended to have lower temporal stability in water quality concentrations. This may be due to the larger amount of pollutants generated by more developed and densely populated regions; these pollutants lead to greater variabilities in water quality. Topographic characteristics also impact the aquatic environment (Yu et al., 2016). Elevation was found to be related to the MRD and ITS values for DO, indicating that elevation weakly influenced the temporal stability of surface water quality. The DO concentration was relatively temporally stable in high-altitude areas, compared to low altitude areas. This is consistent with the relationship between elevation and water quality in Zhejiang Province (Gu et al., 2014; Gu et al., 2015). Meteorological factors, especially rainfall, contribute to variability in water quality (Min and Shibata, 2015). However, precipitation was not correlated with the temporal stability indices for the four indicators in this study. This may be because the difference in precipitation across the study area was not significant enough to influence the variability in water quality between different locations. The lack of correlation may also be because precipitation can have either positive or negative influence on the condition of receiving water bodies (Whitehead et al., 2009), leading to an indeterminate relationship between them.

Table 3 Pearson correlation coefficients between the temporal stability metrics and potential influencing factors.

		Forest (%)	Built-up (%)	Agricultural land (%)	Water (%)	GDP	Population density	Elevation	Precipitation
DO	MRD	0.529 "	-0.485 "	-0.372′	0.355′	-0.464 "	-0.447 "	0.354′	-0.252
	SDRD	0.030	-0.072	0.022	-0.118	0.332′	-0.032	-0.255	0.088
	ITS	-0.292	0.095	0.322′	0.078	0.197	-0.034	-0.337′	0.166
COD_{Mn}	MRD	-0.466 "	0.400′	0.397′	0.115	0.355′	0.097	-0.276	0.252
	SDRD	-0.255	0.019	0.334′	0.027	0.193	0.356′	-0.072	0.241
	ITS	0.028	-0.141	0.122	-0.367′	0.329′	-0.097	0.067	-0.054
TP	MRD	-0.456 "	0.359′	0.441 "	0.020	0.076	-0.039	-0.168	-0.013
	SDRD	-0.331′	0.184	0.392′	-0.112	0.340′	0.349′	-0.123	0.198
	ITS	-0.019	-0.176	0.179	-0.236	-0.033	-0.151	-0.107	0.015
NH_3-N	MRD	-0.482 "	0.514 "	0.365′	0.121	0.339′	0.025	-0.298	0.070
	SDRD	-0.505 "	0.460 "	0.379′	0.310	0.133	0.362′	-0.258	0.199
	ITS	-0.204	0.246	0.142	0.050	-0.089	-0.090	-0.058	-0.174

′ $p < 0.05$

" $p < 0.01$

3.5 Methodological prospects

This study adopted a temporal stability analysis approach, combining a non-parametric correlation test and relative difference analysis. The goal was to characterize the temporal

stability of water quality indicators. The TSA method has considerable potential for investigating the spatio-temporal pattern of surface water quality, and to optimize the distribution of monitoring stations making up water quality monitoring networks. The results demonstrated the feasibility of the TSA method for characterizing the temporal stability of surface water quality. The findings can support water management, by providing knowledge to support the identification of representative monitoring sites.

This approach was designed to support a soil moisture analysis; however, the approach also shows promise in being applied to other measurements (Douaik et al., 2006; Pachepsky et al., 2018; Ran et al., 2015; Stocker et al., 2018). Water quality experiences both temporal changes and spatial variations, and also temporal changes in the spatial pattern. The Spearman's rank correlation of each pair of sampling time was assessed to examine the temporal persistence of site ranks, before applying the temporal analysis of relative differences. The rank correlation coefficient involves the analysis of temporal stability on a regional scale, i.e. the temporal similarity of water quality spatial patterns. In contrast, MRD and SDRD investigate temporal stability on a location scale, i.e. the deviation of individual sites associated with the regional mean.

Studies focusing on optimizing water quality monitoring sites have generally applied clustering methods or dimensionality reduction approaches. To reduce the number of monitoring sites, all sites are clustered into groups based on similarities in water quality measures. Representative sites are then selected from each group (Gu et al., 2015; Hussain et al., 2008). To reduce the number of monitoring indicators, factor analysis/PCA is used to determine the contributions of different water quality indicators. The most important

indicators are identified to be focused on in future monitoring (Su et al., 2011). In contrast with these studies, this study evaluated the relative differences in the concentrations, instead of classifying the sampling sites into groups. This method was not developed to replace the previous approaches; rather, the new approach can play a complementary and assistive role.

3.6 Implication for optimal field monitoring

Based on the theory of temporal stability analysis, this study provides technical support for governmental agencies, so they can optimize water quality monitoring programs and improve water resource management. The temporally stable locations are potential monitoring sites that can be used to estimate mean water quality concentrations for the whole area. In many situations, average water quality levels are used to assess and understand water quality conditions in specific regions. Usually, the arithmetic means are calculated across all monitoring sites to represent the mean values. TSA results can inform innovative methods that adjust mean concentrations to be more logical and representative. For example, more temporally stable sites may be selected to calculate mean concentrations, instead of all monitoring sites. TSA results can be used to optimize the water quality monitoring network, by reducing the number of monitoring locations. The temporally stable sites may be better for reflecting regional water quality conditions over time. In addition, monitoring sites that yield measurements that are consistently higher or lower than the mean levels should be specifically controlled or protected. The TSA results can also be applied to guide the temporal frequencies of the sampling schedule. The pattern of water quality distribution may vary over seasons. If the main purpose is to monitor mean water quality dynamics, data collection can

be less frequent during the seasons with high temporal stability, compared with the frequency during the season with low temporal stability.

The sites with low temporal stability should also be considered (Stocker et al., 2018). Understanding the causes of the large variability in water quality concentrations is important in informing the development of water quality regulations and for pollution control (Gu et al., 2014). The temporally unstable locations may offer insights into the factors influencing the variability in water quality. These insights can help improve current management practices. For example, built-up land and agricultural land were identified as the major factors responsible for the temporal instability of water quality in the study area.

Decreasing the number of monitoring stations, without significantly losing valuable information, benefits long-term water quality monitoring programs. This is particularly the case in large scale systems, which require many monitoring stations that are expensive to build and difficult to maintain (Storey et al., 2011). Study results indicate it is not necessary to monitor all time-stable sites, because water quality at these locations can be estimated by monitoring the temporally stable sites. For example, the DO concentration at site 29 was temporally stable, and was closely correlated with the DO concentration at site 35 (R^2=0.914, p<0.01) (Fig. 9a). The DO concentrations at site 29 between September 2018 and August 2019 were estimated from the observations at station 35. The estimated values effectively fit the measured concentrations at site 29 (R^2=0.807, p<0.01) (Fig. 9b). In this study, most stable locations were distributed in the south. This indicated that fewer monitoring sites may be needed to assess water quality condition in this region, compared to the northern area.

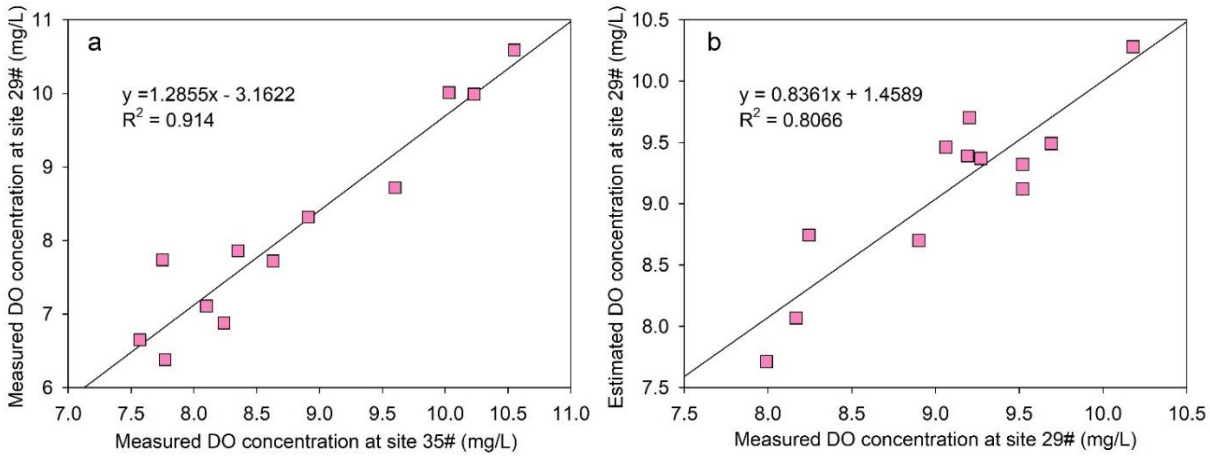

507

508 **Fig. 9** Predicting the DO concentrations at a temporally stable site from a monitored
509 time-stable site. (a) The DO concentrations at site 29 were significantly correlated with
510 concentrations at site 35 between September 2017 and August 2018. (b) The estimated DO
511 concentrations at site 29 effectively fit the measured concentrations between September 2018
512 and August 2019.

513

514 ## 4 Summary and conclusions

515 This study investigated a series of spatio-temporal water quality patterns, using four
516 specific indicators, and identified representative sampling sites in the Qiantang River in
517 China. The temporal stability analysis approach, combining a non-parametric correlation test
518 and relative difference analysis, was used to characterize temporal stability for the four
519 indicators. The results indicated that the spatial pattern of water quality was strongly stable
520 over time. The TP concentration was the most consistent over time among all four indicators.
521 The time-related drift in temporal stability indicated that the spatial distribution of water
522 quality can be maintained for a short period but cannot be sustained for a long period. The
523 SDRD measure was used to identify the most representative site for DO. The SDRD, MABE,

and RMSE measures were used to collectively select the representative locations for COD_{Mn}. The index of temporal stability (ITS) was used to identify the representative sites for TP and NH_3-N.

In this study, SDRD and ITS more efficiently identified representative monitoring sites compared with MABE and RMSE. The identified representative sites estimated the mean concentrations with acceptable errors. The temporal stability was driven by the amount of land use occupied by forest (%), built-up land (%), and agricultural land (%), and by GDP and population density. The spatial pattern of water quality was more temporally stable in the regions where there was more forest and less built-up land and agricultural land. Regions with higher GDP and population density tended to have lower temporal stabilities with respect to water quality. The study found that the TSA method is effective and promising for characterizing the variability in water quality. It also effectively identifies representative sampling sites for optimizing water quality monitoring networks.

Author Contributions Not applicable.

Funding The research was supported by the National Natural Science Foundation of China (Grant No. 41601024 and 41661079).

Data Availability Data are available on request.

Code Availability Not applicable.

Declarations

Ethics Approval Not applicable.

Consent to Participate All authors are informed and consent to participate.

Consent for Publication All authors consent to the publication.

Conflict of Interest None

References

Al-Zahrani, M.A.,Moied, K., 2003. Optimizing water quality monitoring stations using genetic algorithms. Arab. J. Sci. Eng. 28, 57-75.

Behmel, S., Damour, M., Ludwig, R.,Rodriguez, M., 2016. Water quality monitoring strategies-A review and future perspectives. Sci. Total Environ. 571, 1312-1329.

Bu, H., Wei, M., Yuan, Z.,Wan, J., 2014. Relationships between land use patterns and water quality in the Taizi River basin, China. Ecol. Indic. 41, 187-197.

Colliander, A., Jackson, T.J., Bindlish, R., Chan, S., Das, N., Kim, S., Cosh, M., Dunbar, R., Dang, L.,Pashaian, L., 2017. Validation of SMAP surface soil moisture products with core validation sites. Remote Sens. Environ. 191, 215-231.

Cosh, M.H., Jackson, T.J., Bindlish, R.,Prueger, J.H., 2004. Watershed scale temporal and spatial stability of soil moisture and its role in validating satellite estimates. Remote Sens. Environ. 92, 427-435.

Cosh, M.H., Jackson, T.J., Moran, S.,Bindlish, R., 2008. Temporal persistence and stability of surface soil moisture in a semi-arid watershed. Remote Sens. Environ. 112, 304-313.

Cosh, M.H., Jackson, T.J., Starks, P.,Heathman, G., 2006. Temporal stability of surface soil moisture in the Little Washita River watershed and its applications in satellite soil moisture product validation. J. Hydrol. 323, 168-177.

Crow, W.T., Berg, A.A., Cosh, M.H., Loew, A., Mohanty, B.P., Panciera, R., de Rosnay, P., Ryu, D.,Walker, J.P., 2012. Upscaling sparse ground-based soil moisture observations for the validation of coarse-resolution satellite soil moisture products. Rev. Geophys. 50.

570 Dixon, W., Smyth, G.K.,Chiswell, B., 1999. Optimized selection of river sampling sites. Water
571 Res. 33, 971-978.
572 Dorigo, W., Wagner, W., Hohensinn, R., Hahn, S., Paulik, C., Xaver, A., Gruber, A., Drusch,
573 M., Mecklenburg, S.,Oevelen, P.v., 2011. The International Soil Moisture Network: a data
574 hosting facility for global in situ soil moisture measurements. Hydrol. Earth Syst. Sc. 15,
575 1675-1698.
576 Douaik, A., Van Meirvenne, M.,Toth, T., 2006. Temporal stability of spatial patterns of soil
577 salinity determined from laboratory and field electrolytic conductivity. Arid Land Res.
578 Manag. 20, 1-13.
579 EPB, P., 2002. Environmental Quality Standards for Surface Water (GB 3838–2002).
580 Environmental Protection Bureau, Beijing.
581 Gao, X., Wu, P., Zhao, X., Wang, J., Shi, Y., Zhang, B., Lei, T.,Li, H., 2013. Estimation of
582 spatial soil moisture averages in a large gully of the Loess Plateau of China through
583 statistical and modeling solutions. J. Hydrol. 486, 466-478.
584 Glasgow, H.B., Burkholder, J.M., Reed, R.E., Lewitus, A.J.,Kleinman, J.E., 2004. Real-time
585 remote monitoring of water quality: a review of current applications, and advancements in
586 sensor, telemetry, and computing technologies. J. Exp. Mar. Biol. Ecol. 300, 409-448.
587 Grayson, R.B.,Western, A.W., 1998. Towards areal estimation of soil water content from point
588 measurements: time and space stability of mean response. J. Hydrol. 207, 68-82.
589 Gu, Q., Deng, J., Wang, K., Lin, Y., Li, J., Gan, M., Ma, L.,Hong, Y., 2014. Identification and
590 assessment of potential water quality impact factors for drinking-water reservoirs. Int. J.
591 Env. Res. Pub. He. 11, 6069-6084.
592 Gu, Q., Hu, H., Ma, L., Sheng, L., Yang, S., Zhang, X., Zhang, M., Zheng, K.,Chen, L., 2019.
593 Characterizing the spatial variations of the relationship between land use and surface water
594 quality using self-organizing map approach. Ecol. Indic. 102, 633-643.

595 Gu, Q., Wang, K., Li, J., Ma, L., Deng, J., Zheng, K., Zhang, X.,Sheng, L., 2015.
596 Spatio-temporal trends and identification of correlated variables with water quality for
597 drinking-water reservoirs. Int. J. Env. Res. Pub. He. 12, 13179-13194.
598 Hu, W., Shao, M.G.,Reichardt, K., 2010. Using a new criterion to identify sites for mean soil
599 water storage evaluation. Soil Sci. Soc. Am. J. 74, 762.
600 Hussain, M., Ahmed, S.M.,Abderrahman, W., 2008. Cluster analysis and quality assessment of
601 logged water at an irrigation project, eastern Saudi Arabia. J. Environ. Manage. 86,
602 297-307.
603 Icaga, Y., 2005. Genetic algorithm usage in water quality monitoring networks optimization in
604 Gediz (Turkey) river basin. Environ. Monit. Assess. 108, 261-277.
605 Jackson, T.J., Bindlish, R., Cosh, M.H., Zhao, T., Starks, P.J., Bosch, D.D., Seyfried, M.,
606 Moran, M.S., Goodrich, D.C.,Kerr, Y.H., 2012. Validation of Soil Moisture and Ocean
607 Salinity (SMOS) soil moisture over watershed networks in the US. IEEE T. Geosci.
608 Remote. 50, 1530-1543.
609 Jacobs, J.M., Mohanty, B.P., Hsu, E.-C.,Miller, D., 2004. SMEX02: Field scale variability,
610 time stability and similarity of soil moisture. Remote Sens. Environ. 92, 436-446.
611 Kohonen, T., 1990. The self-organizing map. Proceedings of the IEEE. 1, 1-6.
612 Lee, S.W., Hwang, S.J., Lee, S.B., Hwang, H.S.,Sung, H.C., 2009. Landscape ecological
613 approach to the relationships of land use patterns in watersheds to water quality
614 characteristics. Landscape and Urban Planning. 92, 80-89.
615 Martínez-Fernández, J.,Ceballos, A., 2003. Temporal stability of soil moisture in a large-field
616 experiment in Spain. Soil Sci. Soc. Am. J. 67, 1647-1656.
617 Meneses, B.M., Reis, R., Vale, M.J.,Saraiva, R., 2015. Land use and land cover changes in
618 Zêzere watershed (Portugal) - Water quality implications. Sci. Total Environ. 527-528,
619 439-447.

620 Min, F.,Shibata, H., 2015. Simulation of watershed hydrology and stream water quality under
621 land use and climate change scenarios in Teshio River watershed, northern Japan. Ecol.
622 Indic. 50, 79-89.
623 Nasirudin, M.A., Za'bah, U.N.,Sidek, O., 2011. Fresh water real-time monitoring system based
624 on wireless sensor network and GSM, pp. 354-357, IEEE.
625 Neves, H.H.d., Mata, M.G.F.d., Guerra, J.G.M., Carvalho, D.F.d., Wendroth, O.O.,Ceddia,
626 M.B., 2017. Spatial and temporal patterns of soil water content in an agroecological
627 production system. Sci. Agr. 74, 383-392.
628 Ouyang, Y., 2005. Evaluation of river water quality monitoring stations by principal
629 component analysis. Water Res. 39, 2621-2635.
630 Pachepsky, Y., Kierzewski, R., Stocker, M., Sellner, K., Mulbry, W., Lee, H.,Kim, M., 2018.
631 Temporal stability of Escherichia coli concentrations in waters of two irrigation ponds in
632 Maryland. Applied and Environmental Microbiology. 84, e01876-01817.
633 Park, Y.-S., Kwon, Y.-S., Hwang, S.-J.,Park, S., 2014. Characterizing effects of landscape and
634 morphometric factors on water quality of reservoirs using a self-organizing map. Environ.
635 Modell. Softw. 55, 214-221.
636 Peng, J., Loew, A., Merlin, O.,Verhoest, N.E., 2017. A review of spatial downscaling of
637 satellite remotely sensed soil moisture. Rev. Geophys. 55, 341-366.
638 Qi, W., 2006. Technical Explanations for Technical Specifications Requirements for
639 Monitoring of Surface Water and Waste Water (HJ/T 91-2002). Environmental
640 Monitoring in China.
641 Quinn, N.W., Ortega, R., Rahilly, P.J.,Royer, C.W., 2010. Use of environmental sensors and
642 sensor networks to develop water and salinity budgets for seasonal wetland real-time water
643 quality management. Environ. Modell. Softw. 25, 1045-1058.

644 Ran, Y., Li, X., Ge, Y., Lu, X.,Lian, Y., 2015. Optimal selection of groundwater-level
645 monitoring sites in the Zhangye Basin, Northwest China. J. Hydrol. 525, 209-215.
646 Stocker, M.D., Penrose, M.,Pachepsky, Y.A., 2018. Spatial patterns of Escherichia coli
647 concentrations in sediment before and after high-flow events in a first-order creek. J.
648 Environ. Qual. 47, 958-966.
649 Storey, M.V., Van der Gaag, B.,Burns, B.P., 2011. Advances in on-line drinking water quality
650 monitoring and early warning systems. Water Res. 45, 741-747.
651 Strobl, R.O.,Robillard, P.D., 2008. Network design for water quality monitoring of surface
652 freshwaters: A review. 87, 639-648.
653 Su, S., Li, D., Zhang, Q., Xiao, R., Huang, F.,Wu, J., 2011. Temporal trend and source
654 apportionment of water pollution in different functional zones of Qiantang River, China.
655 Water Res. 45, 1781-1795.
656 Sur, C., Jung, Y.,Choi, M., 2013. Temporal stability and variability of field scale soil moisture
657 on mountainous hillslopes in Northeast Asia. Geoderma. 207, 234-243.
658 Vachaud, G., Passerat de Silans, A., Balabanis, P.,Vauclin, M., 1985. Temporal Stability of
659 Spatially Measured Soil Water Probability Density Function 1. Soil Sci. Soc. Am. J. 49,
660 822-828.
661 Van Pelt, R.S.,Wierenga, P.J., 2001. Temporal stability of spatially measured soil matric
662 potential probability density function. Soil Sci. Soc. Am. J. 65, 668-677.
663 Wagner, W., Pathe, C., Doubkova, M., Sabel, D., Bartsch, A., Hasenauer, S., Blöschl, G.,
664 Scipal, K., Martínez-Fernández, J.,Löw, A., 2008. Temporal stability of soil moisture and
665 radar backscatter observed by the Advanced Synthetic Aperture Radar (ASAR). Sensors.
666 8, 1174-1197.

667 Whitehead, P.G., Wilby, R.L., Battarbee, R.W., Kernan, M.,Wade, A.J., 2009. A review of the
668 potential impacts of climate change on surface water quality. Hydrological Sciences
669 Journal. 54, 101-123.
670 Wu, Y.,Chen, J., 2013. Investigating the effects of point source and nonpoint source pollution
671 on the water quality of the East River (Dongjiang) in South China. Ecol. Indic. 32,
672 294-304.
673 Yu, S., Xu, Z., Wei, W.,Zuo, D., 2016. Effect of land use types on stream water quality under
674 seasonal variation and topographic characteristics in the Wei River basin, China. Ecol.
675 Indic. 60, 202-212.
676 Zhang, P.,Shao, M.a., 2013. Temporal stability of surface soil moisture in a desert area of
677 northwestern China. J. Hydrol. 505, 91-101.
678 Zhao, Y., Peth, S., Wang, X., Lin, H.,Horn, R., 2010. Controls of surface soil moisture spatial
679 patterns and their temporal stability in a semi-arid steppe. Hydrol. Process. 24, 2507-2519.
680 Zhou, P., Huang, J., Jr, P.R.,Hong, H., 2016. New insight into the correlations between land
681 use and water quality in a coastal watershed of China: Does point source pollution weaken
682 it? Sci. Total Environ. 543, 591-600.
683 Zhou, X., Lin, H.,Zhu, Q., 2007. Temporal stability of soil moisture spatial variability at two
684 scales and its implication for optimal field monitoring. Hydrol. Earth Syst. Sci. Discuss. 4,
685 1185-1214.
686

Figures

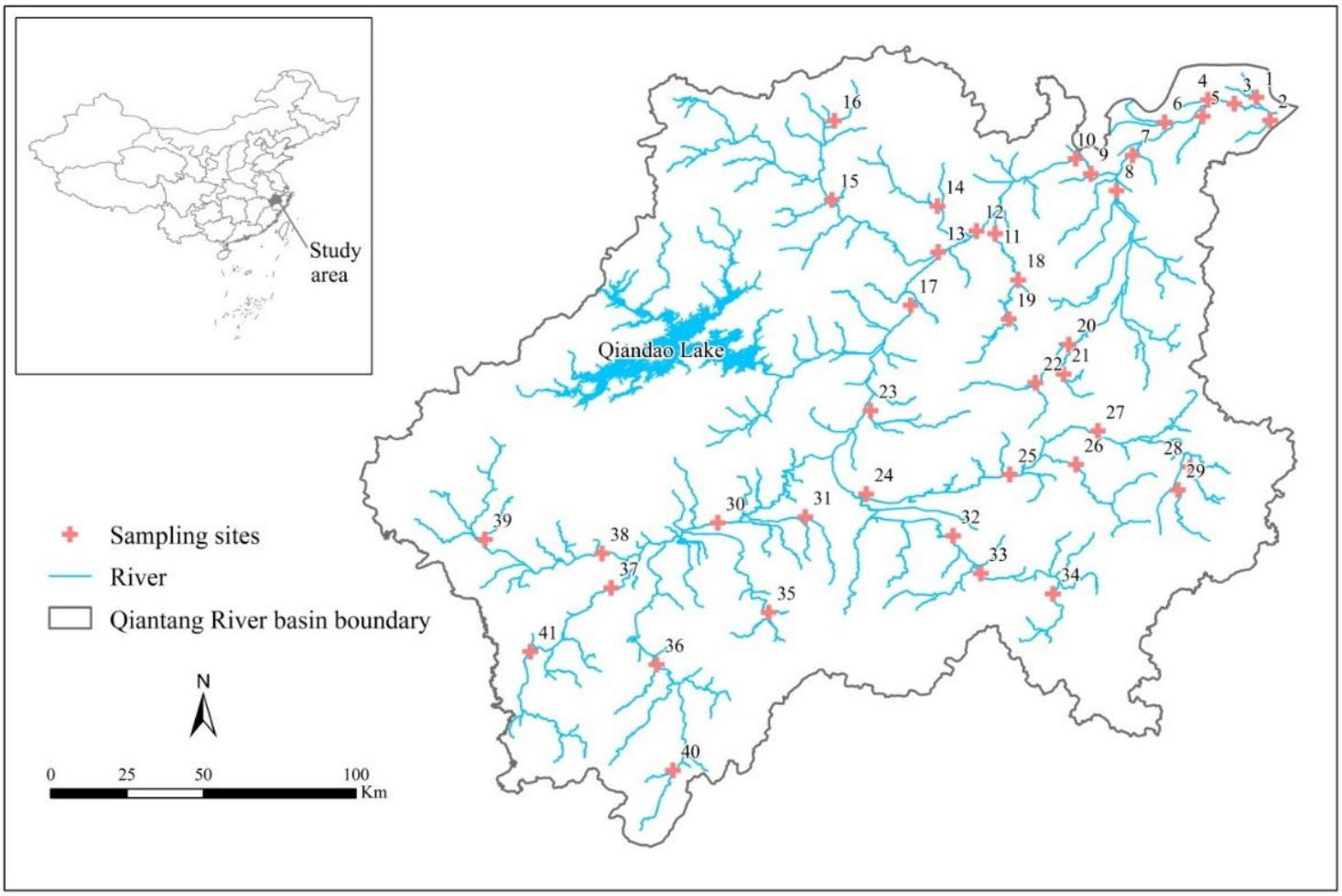

Figure 1

Location of the study area in China and spatial distribution of the monitoring sites. Note: The designations employed and the presentation of the material on this map do not imply the expression of any opinion whatsoever on the part of Research Square concerning the legal status of any country, territory, city or area or of its authorities, or concerning the delimitation of its frontiers or boundaries. This map has been provided by the authors.

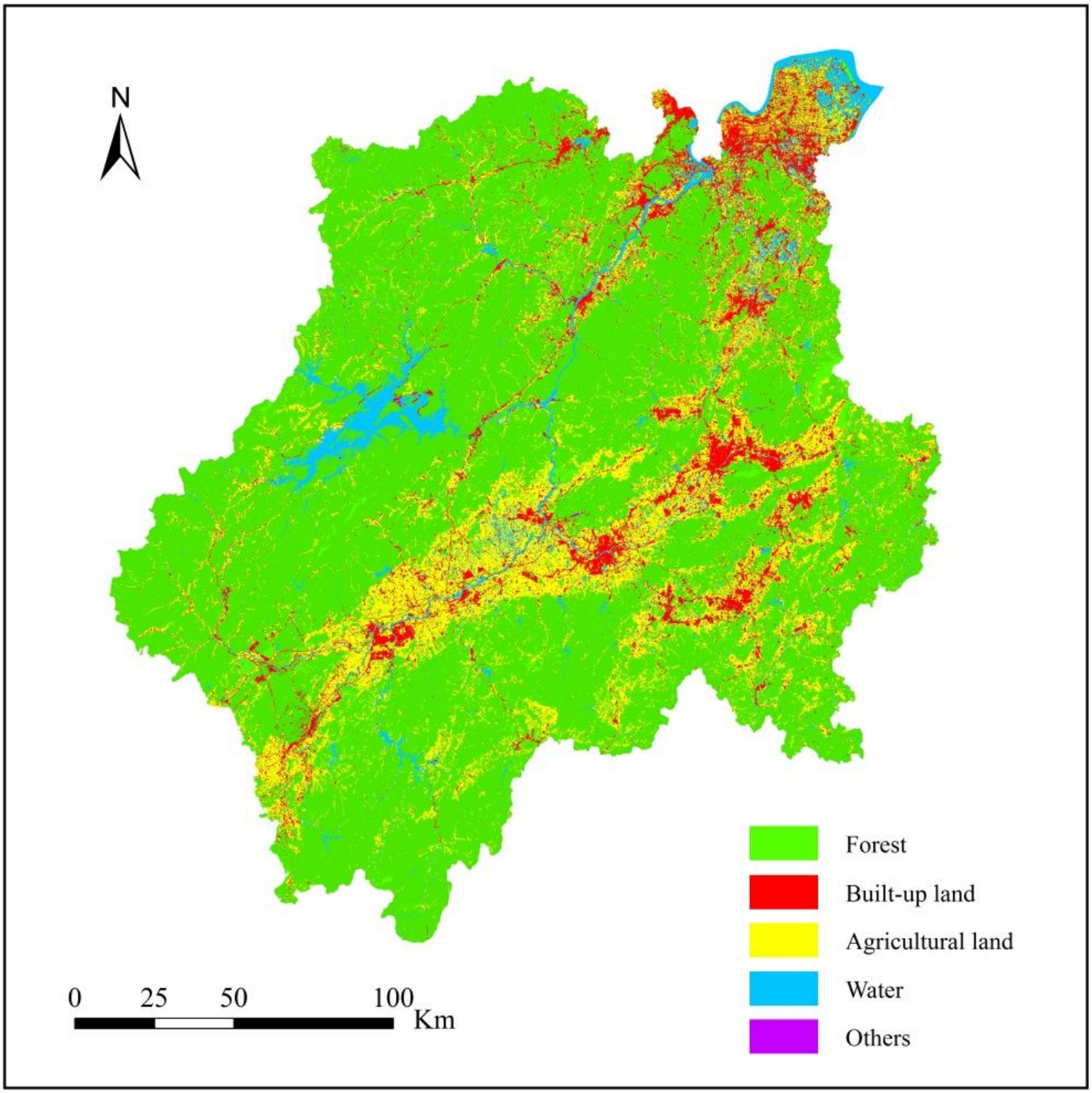

Figure 2

Land use in the Qiantang River basin in 2017. Note: The designations employed and the presentation of the material on this map do not imply the expression of any opinion whatsoever on the part of Research Square concerning the legal status of any country, territory, city or area or of its authorities, or concerning the delimitation of its frontiers or boundaries. This map has been provided by the authors.

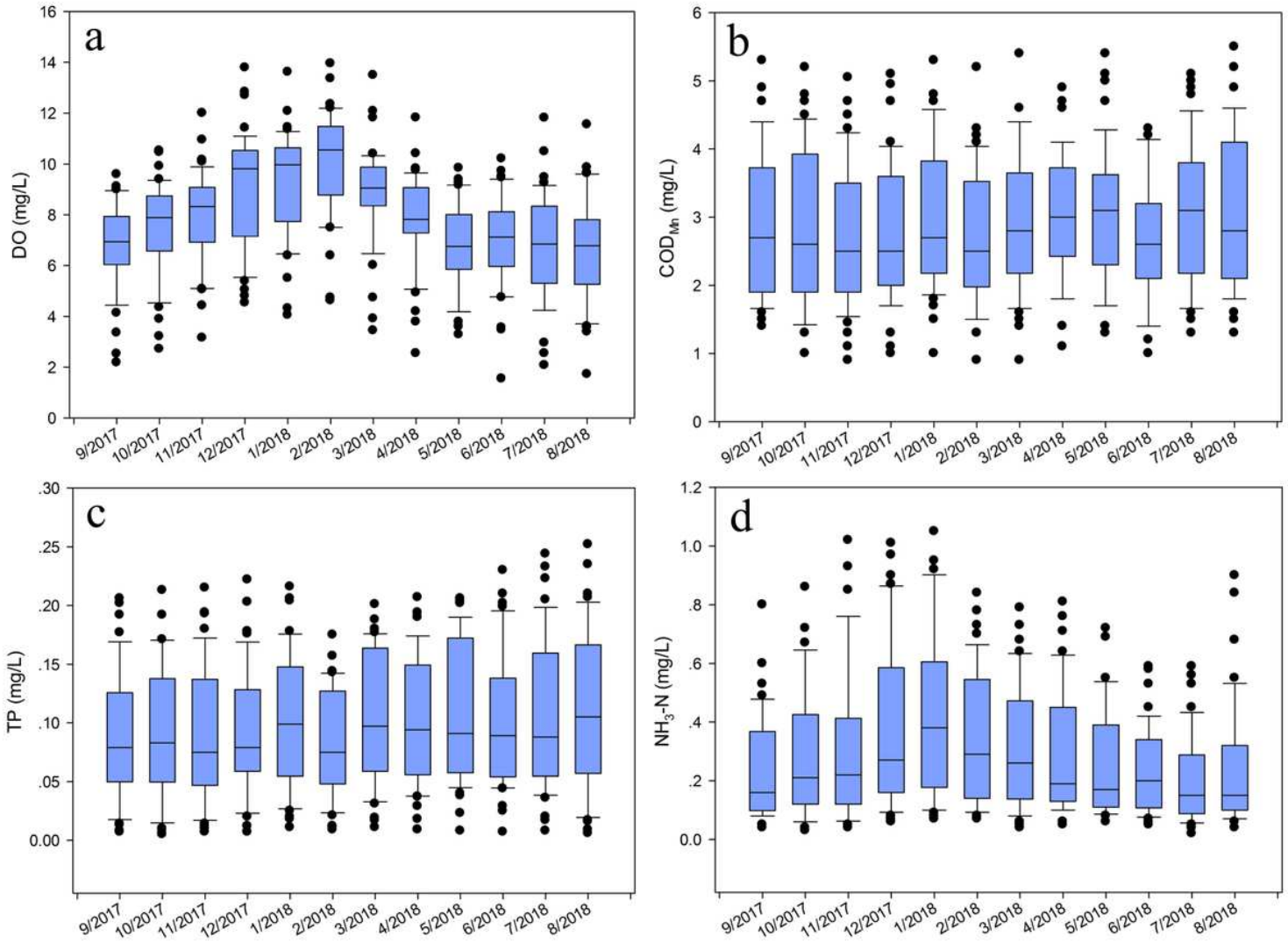

Figure 3

Annual variations in (a) DO, (b) CODMn, (c) TP, and (d) NH3-N between September 2017 and August 2018.

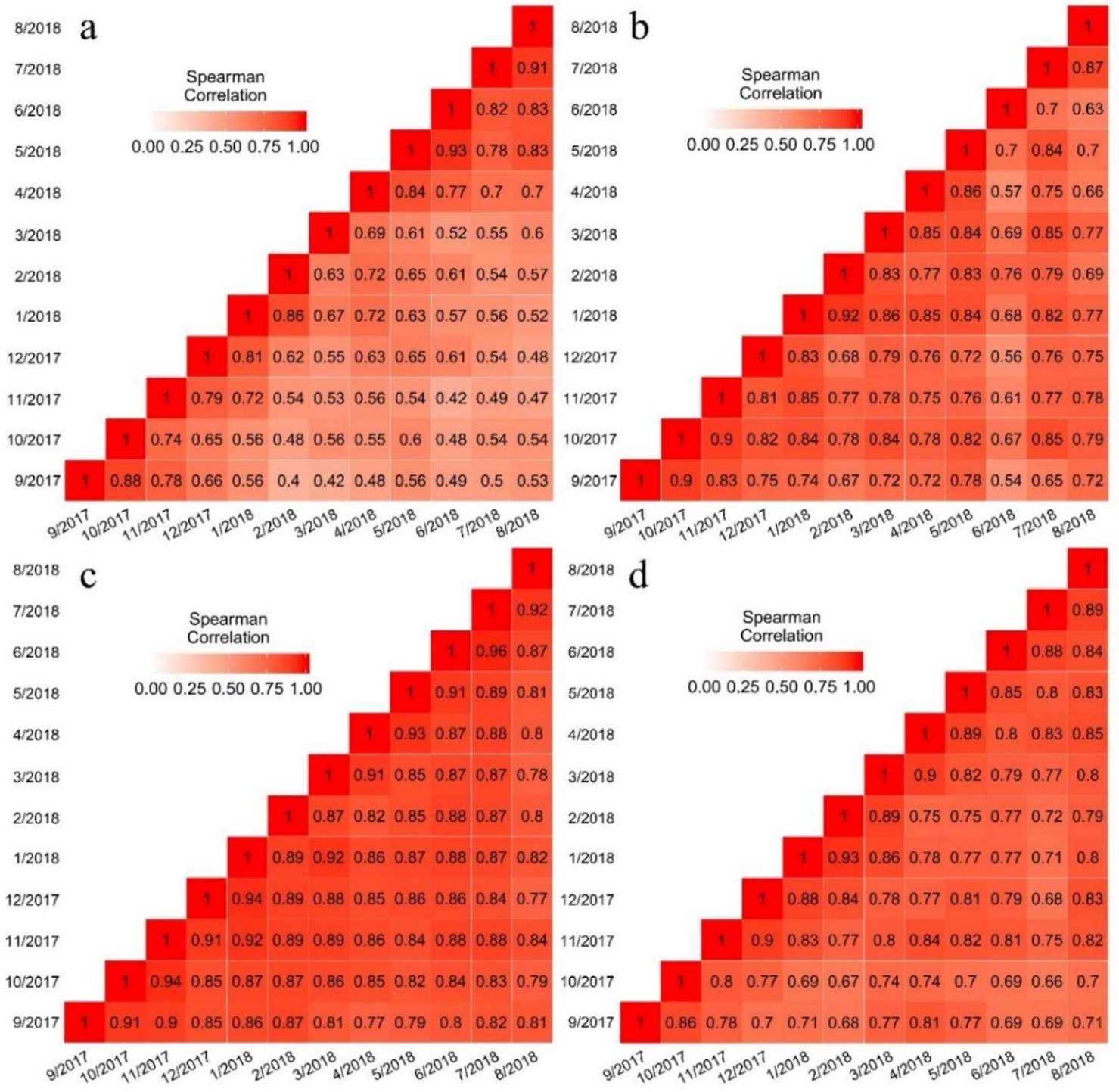

Figure 4

Matrix of Spearman's rank correlation coefficients for the comparisons of water quality concentrations in different months between September 2017 and August 2018: (a) DO, (b) CODMn, (c) TP, and (d) NH3-N. All correlations are statistically significant ($p<0.01$).

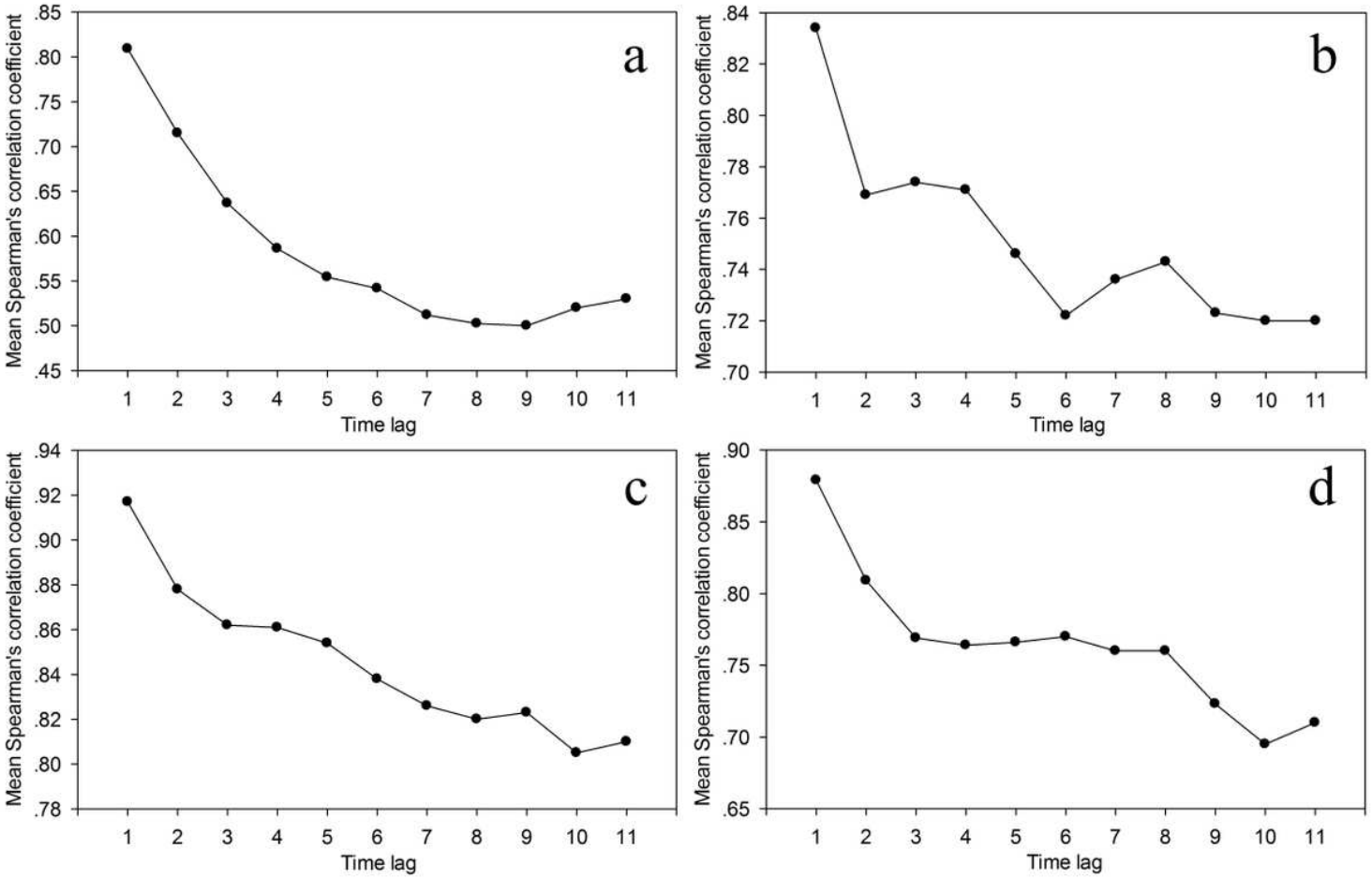

Figure 5

Mean Spearman’s rank correlation coefficient corresponding to different time lags (months) for (a) DO, (b) CODMn, (c) TP, and (d) NH3-N.

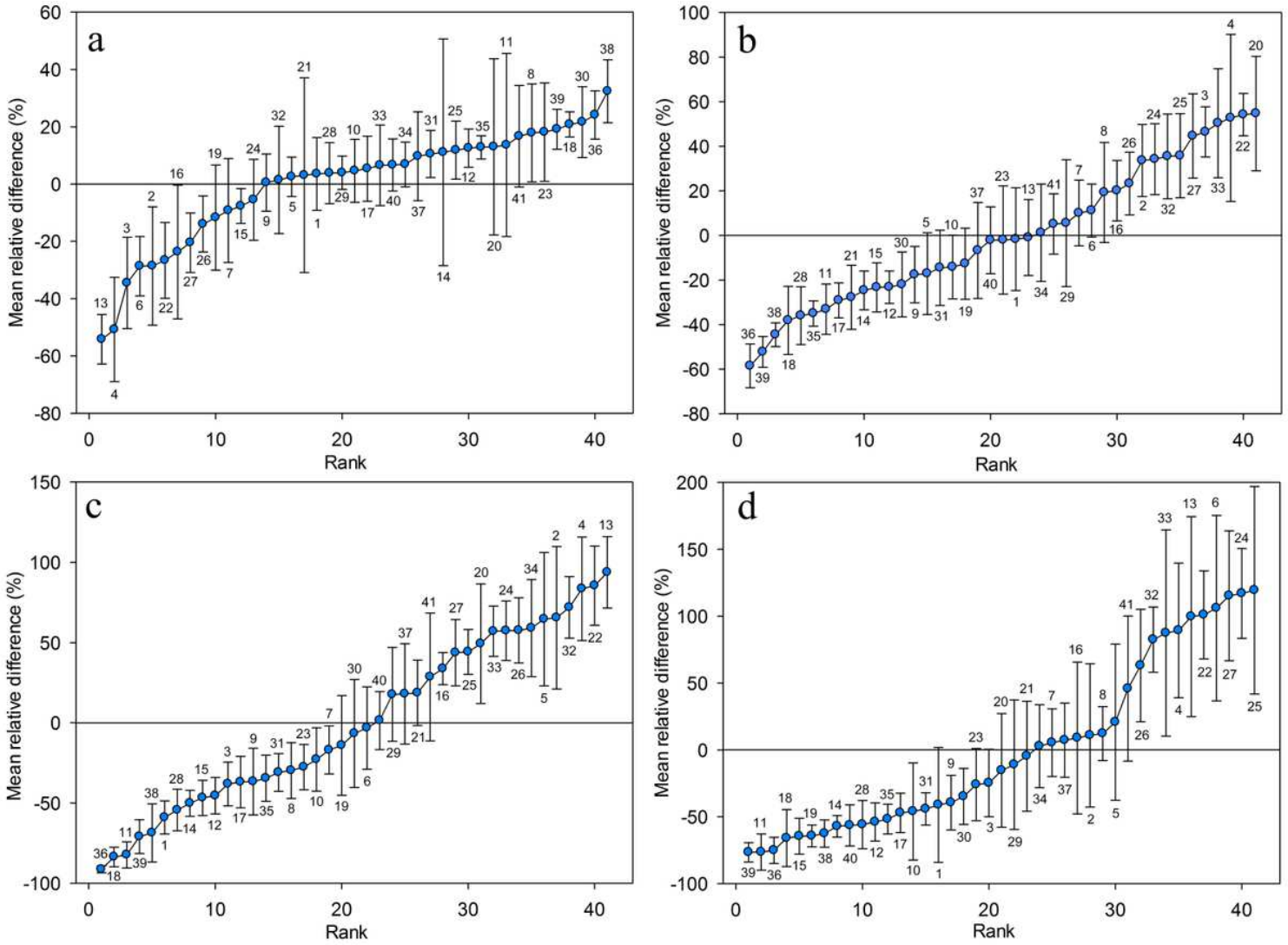

Figure 6

The mean relative difference (MRD) and standard deviation of relative difference (SDRD) of (a) DO, (b) CODMn, (c) TP, and (d) NH3-N. The MRDs are ranked in ascending order; the associated SDRD values are indicated by error bars. The numbers near the bars are the identification numbers of the monitoring sites.

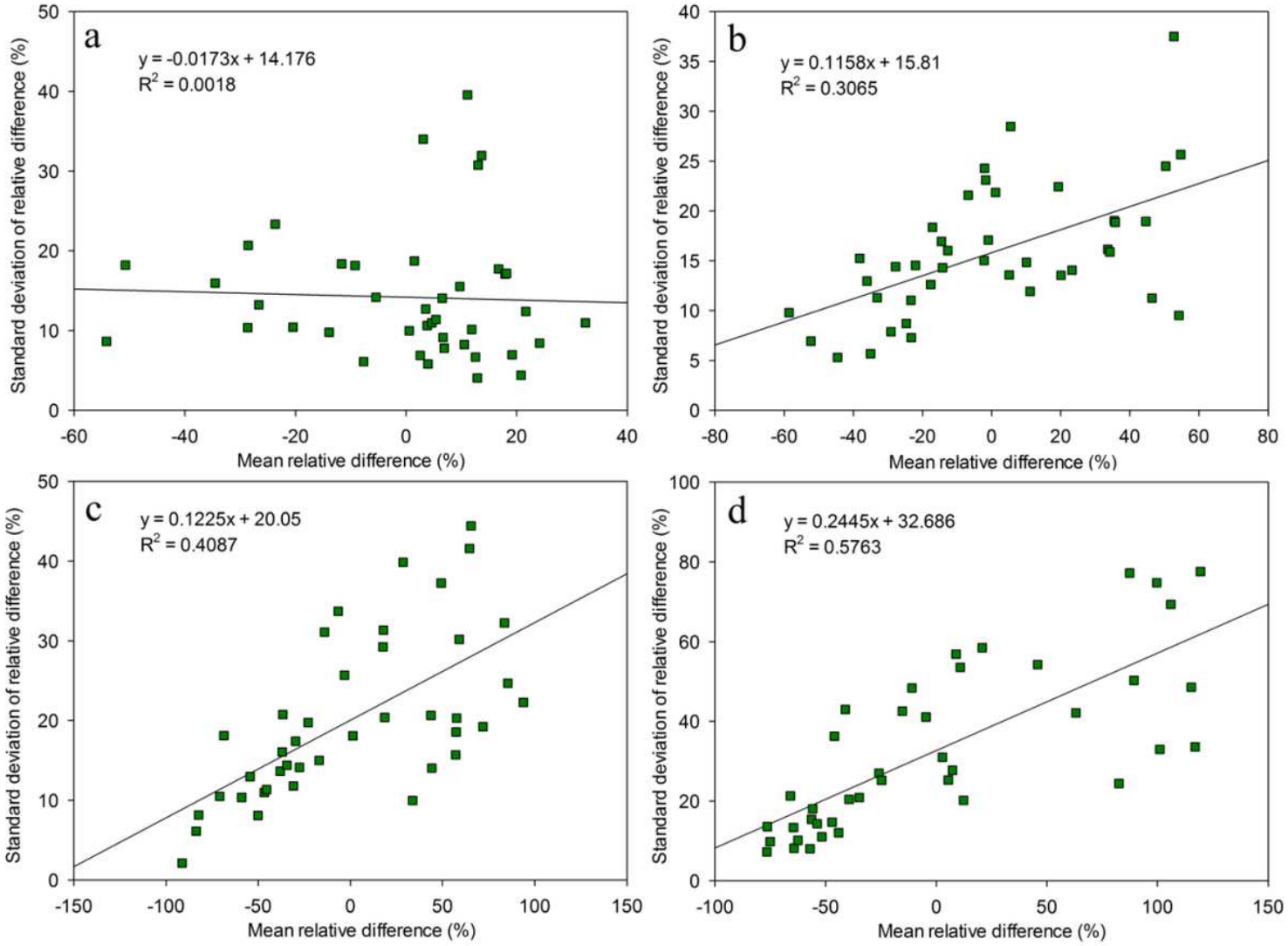

Figure 7

Relationships between the mean relative difference (MRD) and standard deviation of relative difference (SDRD) for (a) DO, (b) CODMn, (c) TP, and (d) NH3-N.

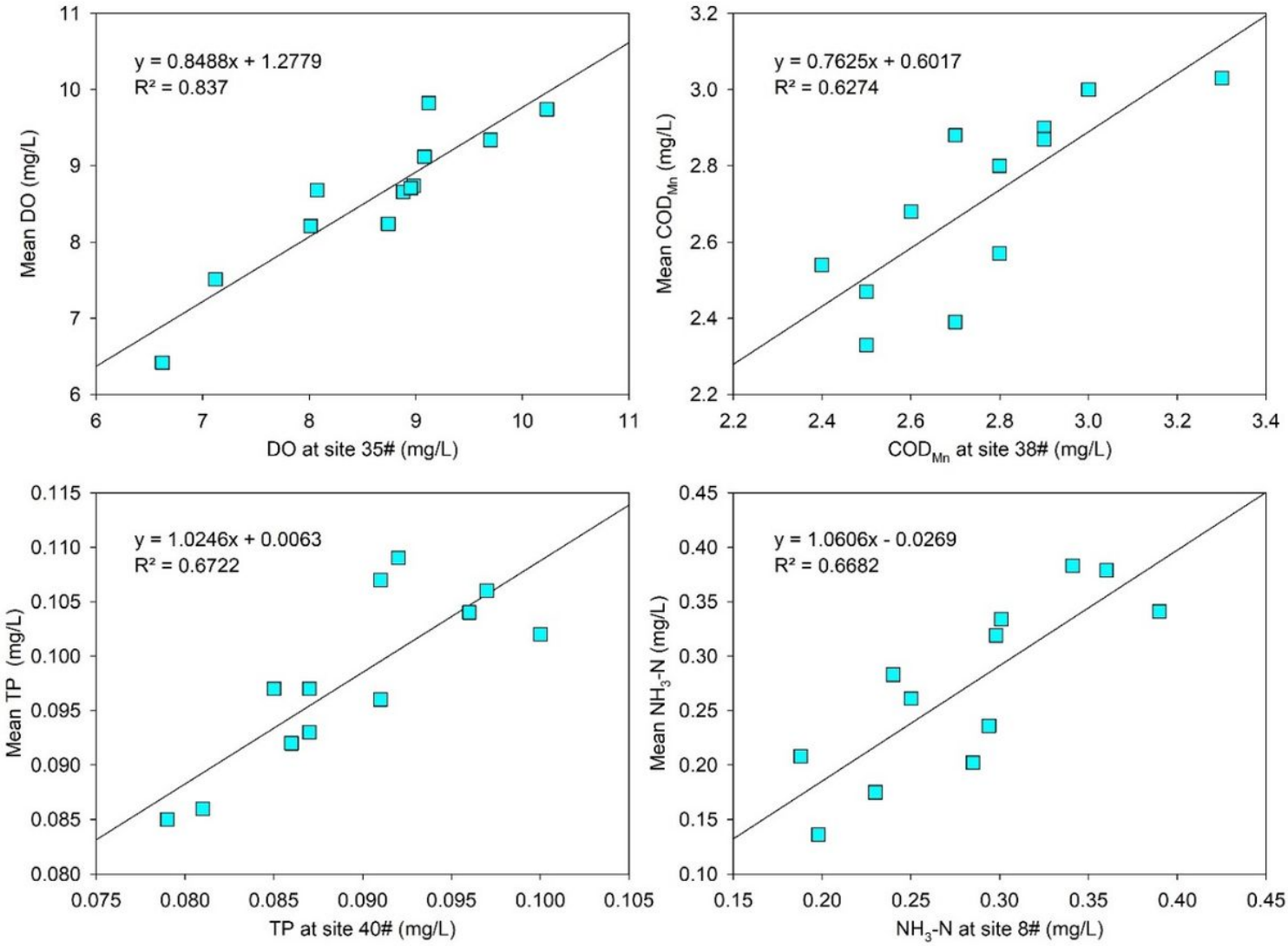

Figure 8

Comparison of water quality concentrations between the total mean values and concentrations of representative sites for DO (site 35), CODMn (site 38), TP (site 40), and NH3-N (site 8), between September 2018 and August 2019.

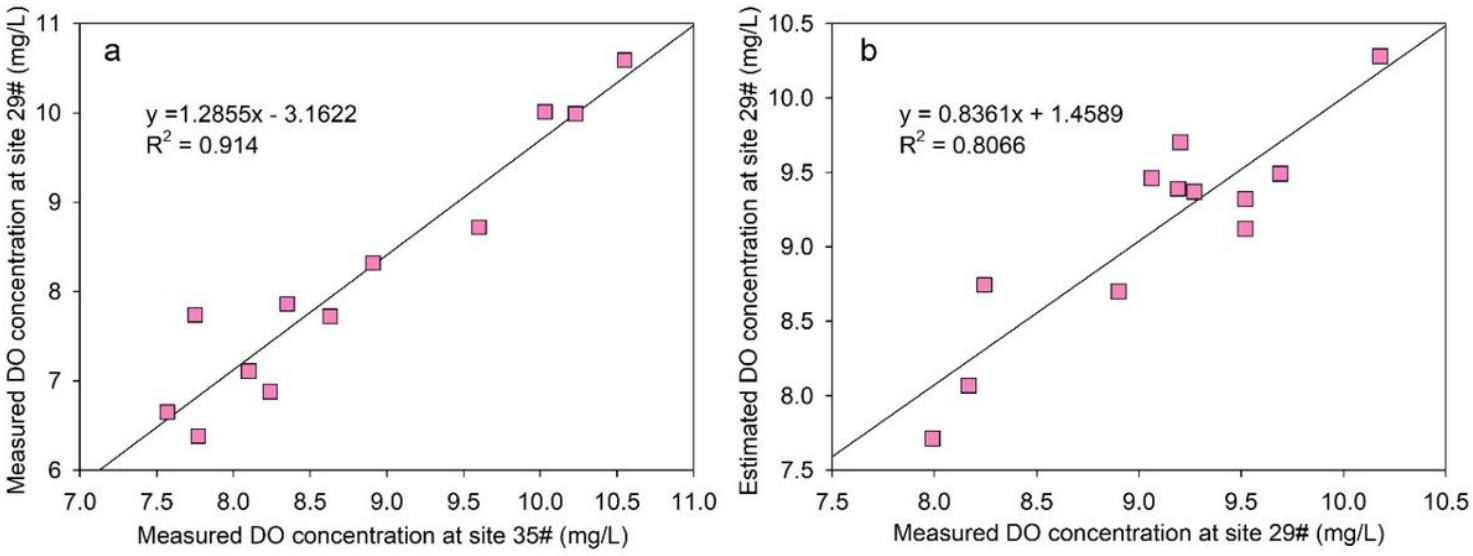

Figure 9

Predicting the DO concentrations at a temporally stable site from a monitored time-stable site. (a) The DO concentrations at site 29 were significantly correlated with concentrations at site 35 between September 2017 and August 2018. (b) The estimated DO concentrations at site 29 effectively fit the measured concentrations between September 2018 and August 2019.